

Fast Off-Board Charger for Electric Vehicles

Faculty of Engineering
Alexandria University

Contents

I	AC/DC Conversion	11
1	Introduction to AC/DC Conversion	13
2	What is Rectification?	15
2.1	Half-Wave Rectification	15
2.2	Full-Wave Rectification	16
3	Topologies for AC/DC Conversion Stage	17
3.1	Three-Phase Passive Rectifier	17
3.2	Three-Phase Vienna Rectifier	18
3.3	Three-Phase Two-Level Six-Switch Boost-Type Rectifier	18
3.4	Three-Phase Three-Level Neutral Point Clamped Converter	19
3.5	Three-Phase Three-Level T-Type Converter	20
4	Implementation of Closed-Loop AC/DC Converter	21
4.1	Proportional Integral Derivative (PID)	22
4.1.1	P-Controller	22
4.1.2	I-Controller	23
4.1.3	D-Controller	23
4.1.4	Tuning of PID Controller	24
4.1.5	The Main Control Circuit	24
4.2	Phase-Locked Loop (PLL)	25
4.2.1	Method I	26
4.2.2	Method II	27
4.3	Clarke and Park Transformations	27
4.3.1	Clarke Transform	28

4.3.2	Park Transform	29
4.4	Filter Design	29
4.4.1	Active Filters	30
4.4.2	Passive Filters	30
	L-type Filter	30
	LC-type Filter	31
	LCL-type Filter	31
4.4.3	Grid-Connected Inverters	31
4.4.4	Method I	32
	Design Example	32
	Simulation	33
4.4.5	Method II	34
	Design Example	35
	Simulation	36
4.4.6	Method III	37
	Design Example	38
	Simulation	39
4.4.7	Method IV	40
	Design Example	41
	Simulation	42
4.4.8	Method V	43
	Design Example	43
	Simulation	44
4.4.9	Comparison	45
4.4.10	Chosen Method	46
	Design Example - Low Power	46
	Design Example - High Power	47
4.5	DC-Link Capacitor Selection	47
4.5.1	Method I	48
4.5.2	Method II	49
4.5.3	Chosen Method	49
	Design Example - Low Power	49

CONTENTS	5
Design Example - High Power	49
4.6 Component Selection	50
4.6.1 The Inverter Module	50
The Features	50
4.6.2 The Current Sensor	51
4.6.3 The Voltage Sensor	51
The Features	51
Interfacing with Micro-controller - Op-Amp Technique	53
4.6.4 The Micro-controller	55
4.7 Hardware Design	55
4.7.1 The Inverter Module	55
4.7.2 DC-Link	57
4.7.3 Current Sensors	58
4.7.4 Voltage Sensors	59
4.7.5 Micro-controller Interfacing	60
Bibliography	60

List of Figures

2.1	Half-wave rectification process	15
2.2	Full-wave rectification process	16
3.1	Three-phase passive rectifier	17
3.2	Three-phase vienna rectifier	18
3.3	Three-phase two-level six-switch boost-type rectifier	19
3.4	Three-phase three-level neutral point clamped converter	19
3.5	Three-phase three-level T-type converter	20
4.1	The implemented model of 10KW system using VOC	21
4.2	The effect of P-gain on a system	22
4.3	PI-control process	23
4.4	PID control on a system	24
4.5	Control circuit of AFE (Active Front-end Rectifier) with 800V output voltage	25
4.6	PI control loop of AFE	26
4.7	PLL control using VOC method	27
4.8	$\alpha - \beta$ signals to d-q signals	27
4.9	ABC frame	28
4.10	Clarke transform	28
4.11	Park transform	29
4.12	Three-phase inverter with passive filter	31
4.13	The output voltage on the DC-link – method I	33
4.14	The current and the phase voltage of phase R – method I	34
4.15	The output voltage on the DC-link – method II	36
4.16	The current and the phase voltage of phase R – method II	37
4.17	The output voltage on the DC-link – method III	39

4.18	The current and the phase voltage of phase R – method III	40
4.19	The output voltage on the DC-link – method IV	42
4.20	The current and the phase voltage of phase R – method IV	42
4.21	The output voltage on the DC-link – method V	44
4.22	The current and the phase voltage of phase R – method V	45
4.23	V_{out} versus I_p plot	51
4.24	The schematic of the supply for the voltage sensor	52
4.25	The internal connection of the voltage sensor	52
4.26	Op-amp circuit	53
4.27	The circuit diagram of the op-amp	54
4.28	The schematic of the op-amp circuit	54
4.29	DSP LaunchpadF28069M	55
4.30	The schematic of the inverter module board	56
4.31	Inverter module hardware board design	56
4.32	The schematic of the DC-link board	57
4.33	DC-link hardware board design	57
4.34	The schematic of the current sensors board	58
4.35	Current sensors hardware board design	58
4.36	The schematic of the voltage sensors board	59
4.37	Voltage sensors hardware board design	59
4.38	The schematic of the DSP interfacing board	60
4.39	DSP interfacing hardware board design	60

List of Tables

4.1	Comparison between the output of different design methods	45
4.2	Recommended connections for different sensitivities	51

Part I

AC/DC Conversion

Chapter 1

Introduction to AC/DC Conversion

The electrical power supplied by wall outlets varies globally, offering either 50Hz or 60Hz AC (Alternating Current) with a nominal voltage of approximately 120VAC or 230VAC. However, for devices like phones and laptops, which run on low voltage DC (Direct Current), an adapter is typically required. Despite the ubiquity of DC-powered electronic equipment, mains power distribution employs AC. Understanding the historical and technical reasons behind this choice provides insight into the development of our modern power systems.

AC gained prominence in distributed networks for several compelling reasons. Firstly, the early AC generators were simpler, leading to rapid improvements in reliability. Secondly, the ability to easily change the voltage using transformers became a pivotal advantage. Lastly, the use of multiple pole alternators reduced the rotation speed of more powerful generators. This three-pronged approach made AC a practical choice for widespread power distribution.

One historical obstacle for DC power distribution was introduced by Thomas Edison, who championed DC systems. Edison faced challenges as he attempted to compete with AC by using generator sets. While low voltage DC motors for step-up purposes were easy to manufacture, high-voltage DC motors for the corresponding step-down process proved unreliable, leading to frequent system breakdowns. In the end, even Edison abandoned the DC distribution concept in favor of alternating current power distribution[1].

The choice of AC over DC also considered the issue of power losses in transmission lines. As more houses were connected to the power grid, the losses in a cable with resistance (I^2R loss) increased. By doubling the voltage, the current could be halved, allowing the same power cable to carry the current four times further. This principle applied to both DC and AC power transmission, but the use of transformers made it more convenient to step up the AC supply voltage for long-distance transmission and step it back down at the destination.

Currently, modern technologies enable efficient bidirectional conversion between AC and DC with high power and efficiency. While AC mains voltages are likely to remain standard soon, there is a growing interest in reconsidering DC power distribution due to our increasing dependence on electrical power. Modern power distribution involves multiple interconnected sources forming a power grid. Transmitting power over long distances ($>500\text{km}$) using high voltage DC has become more appealing because it eliminates impedance losses, and generators do not need to be synchronized to the same frequency or voltage.

For instance, a notable example of high voltage DC power transmission is a 2000MW link con-

necting England and France. This interconnection allows the two countries to exchange power based on domestic demand, highlighting the advantages of high voltage DC in a modern power grid. As technology continues to evolve, the debate between AC and DC power distribution will persist, driven by factors such as efficiency, cost, and the demands of our increasingly interconnected and power-dependent world.

AC/DC converters are the backbone components for expanding and improving the functioning of electrical vehicles (EVs). Primarily, an outlet delivers AC power, whereas EV batteries function with DC power for charging the battery. Thus, there is a need for an AC/DC converter for converting AC power to DC power. It is also the major component of an EV battery charger and enhances the input current shape for power-factor correction and harmonic reduction.

The power range of fast charging is above 50 kW, which is considered high according to industry standards. So there is a need for a larger AC/DC converter to supply this extra power for fast charging. Thus, high-power charging is best carried out where AC/DC converters are built into the charging station and not installed inside the vehicle due to size constraints[2]. We will focus on off-board fast chargers for electric vehicles.

Chapter 2

What is Rectification?

Rectification refers to the process of transforming an alternating current (AC) waveform into a direct current (DC) waveform, producing a signal with a single polarity. It is essential to note that a DC voltage or current does not necessarily have to be constant; it simply means the signal's polarity remains unchanged. In some cases, a varying amplitude DC signal is referred to as pulsating DC.

The concept of rectification is fundamental in modern electronic circuits as many electronic devices require a stable, unvarying DC voltage to power their internal circuitry. Given that residential and commercial power distribution is typically in the form of AC, some form of AC to DC conversion is necessary.

Rectifiers, which perform the conversion of AC to DC, are classified into two categories based on the type of conversion: half-wave rectifiers and full-wave rectifiers. The former involves converting half cycles of AC into DC, while the latter processes full cycles of AC into DC. Understanding the differences between half-wave and full-wave rectifiers, as well as a brief exploration of each type, facilitates a clearer grasp of their distinct functionalities.

2.1 Half-Wave Rectification

A half-wave rectifier is a circuit that transforms only half of the alternating current (AC) cycle into direct current (DC). The typical configuration of a half-wave rectifier involves a semiconductor diode, and the circuit and output waveform are depicted in Figure 2.1.

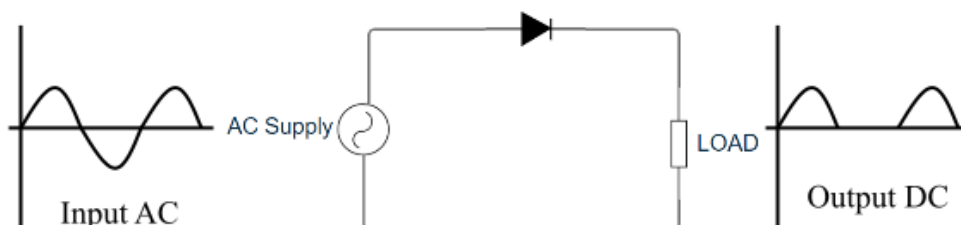


Figure 2.1: Half-wave rectification process

In the process of half-wave rectification, the AC is initially supplied to the diode. Here is how the rectification unfolds: During the positive half cycle of AC, the diode, operating in a forward-biased state, acts as a short circuit, allowing electric current to pass through. Conversely, during the

negative half cycle of AC, the diode becomes reverse-biased, acting as an open circuit and preventing conduction. Consequently, the voltage at the load terminals is present only during the positive half cycle of AC. Thus, the alternating current is converted into direct current, flowing in a single direction, but only during one half cycle of AC.

2.2 Full-Wave Rectification

In contrast to half-wave rectifier, a full-wave rectifier transforms the entire cycle of alternating current into direct current. The circuit for a full-wave rectifier comprises four semiconductor diodes. Two of the four terminals of the diodes are connected to the AC supply, while the other two terminals link to the load resistor.

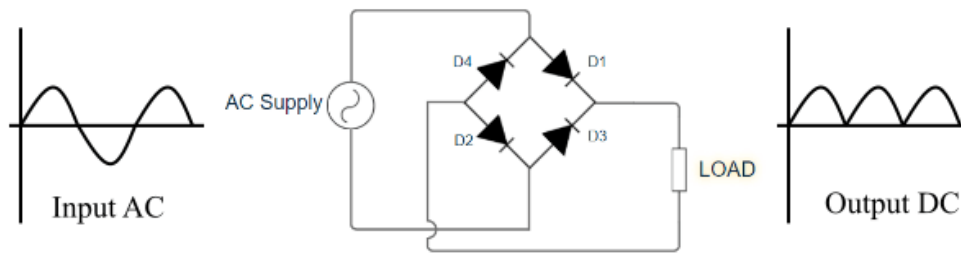


Figure 2.2: Full-wave rectification process

During the positive half cycle of AC, diode D_1 and diode D_2 are forward biased, and diode D_3 and diode D_4 are reverse biased. Consequently, diodes D_1 and D_2 conduct, allowing current to flow through D_1 , D_2 and the load resistor R_L . In the negative half cycle of AC, the situation reverses: diodes D_1 and D_2 become reverse biased, and diodes D_3 and D_4 become forward biased. Only diodes D_3 and D_4 are conducted during this negative half cycle, and the current flows through D_3 , D_4 and the load resistor R_L . The circuit and output voltage waveform for the full-wave rectifier are illustrated in Figure 2.2. This way, a full-wave rectifier efficiently converts the entire AC cycle into DC [3].

While the explanations above focus on a single-phase AC system, they can be extended to three-phase systems commonly used in fast-charging offboard chargers. In a three-phase half-wave rectifier, the system requires three diodes, and for the full-bridge system, six diodes are necessary. The adaptability of rectification principles to different configurations underscores their significance in converting AC to DC, a crucial requirement for many electronic devices and power systems.

Chapter 3

Topologies for AC/DC Conversion Stage

The AC-DC converter of an offboard charger is a front-end rectifier before the DC-DC conversion stage of the complete EV fast charging station. Various topologies are available that convert AC power from the utility grid to DC power. Such topologies are expected to manage high power fed directly to the battery as part of an EV fast charging solution.

3.1 Three-Phase Passive Rectifier

The simplest rectifier configuration is the three-phase diode rectifier, comprising six diodes, AC side inductors, and a DC side capacitor (refer to 3.1).

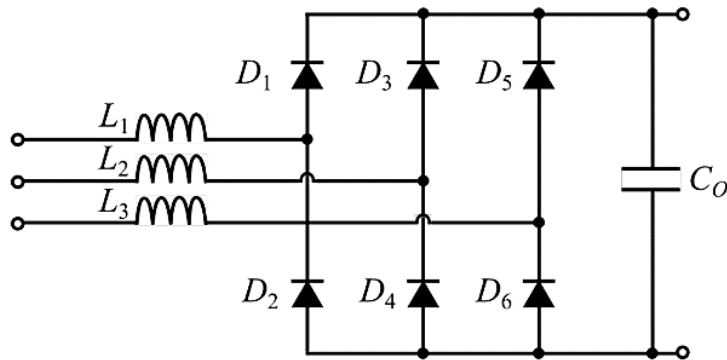


Figure 3.1: Three-phase passive rectifier

As it runs without active switches, this converter drops the need for a control system or gate drivers, streamlining its functionality. Diodes switch at the grid frequency without active current shaping or control over the output voltage. However, diode rectifiers can introduce a Total Harmonic Distortion (THD) of 40–70% into grid currents, potentially stressing the grid, especially with numerous fast high-power passive rectifiers. Due to its lower efficiency, unidirectional power flow, and higher THD, this conventional passive rectifier topology is not recommended for fast charging applications.

Unlike passive rectifiers, active rectifiers, when employed, allow for controlled DC link voltage, keeping the desired voltage level across varying loads. This helps minimize THD, achieving both

high efficiency and power factor. The later comparison focuses on three boost-type bidirectional active converters: Three-phase two-level six-switch boost-type rectifier, Three-phase three-level neutral point clamped converter, and Three-phase three-level T-type converter.

3.2 Three-Phase Vienna Rectifier

The three-phase Vienna rectifier, illustrated in 3.2, includes three input inductors for voltage boosting, followed by six diodes for rectification and six semiconductor switches. Additionally, two split capacitors are incorporated in the output. Its functioning is akin to a traditional three-phase boost Power Factor Correction (PFC) rectifier, but unlike the latter, it does not ease bidirectional power flow. The Vienna rectifier employs a straightforward control mechanism, ensuring unity power factor operation and minimizing Total Harmonic Distortion (THD). Its notable efficiency, particularly in power-dense applications, makes it well-suited for high-power scenarios such as fast-charging Electric Vehicles (EVs).

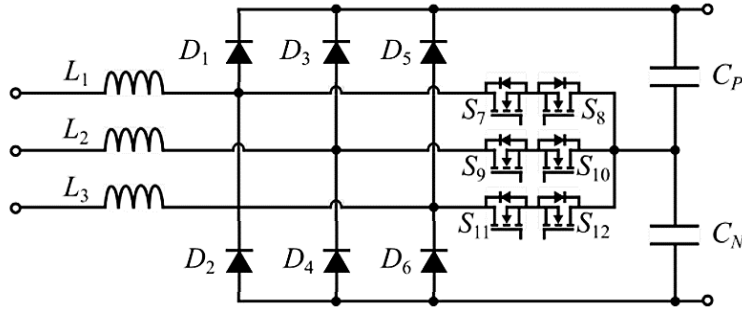


Figure 3.2: Three-phase vienna rectifier

To enable bidirectional power flow, the Vienna rectifier can be changed by replacing diodes with switches, a modification especially beneficial in Vehicle-to-Grid (V2G) applications. The Vienna rectifier typically runs using modulation methods like carrier-based Pulse Width Modulation (PWM), Space Vector PWM, and discontinuous PWM. However, in the case of interleaved Vienna rectifiers, Space Vector PWM can introduce distortions in input current waveforms, while the other two PWM techniques may lead to undesirable ripples. To address these challenges, a hybrid Space Vector PWM approach is employed, effectively mitigating the issues associated with the modulation techniques.

3.3 Three-Phase Two-Level Six-Switch Boost-Type Rectifier

The configuration for the three-phase two-level boost-type rectifier is depicted in 3.3. It forms six active switches (MOSFETs or IGBTs), AC side boost inductors, and a DC side filter capacitor. Known for its simplicity, robustness, and familiarity, the two-level six-switch rectifier topology needs larger-volume input inductors and is constrained by a maximum switching frequency compared to three-level converters.

The rectifier, being of a boosting nature, imposes a lower limit on the DC link voltage. For instance, if the rectifier is connected to a three-phase grid with a 400 V RMS line-to-line voltage, the smallest DC link voltage would be 565 V, equal to the line-to-line voltage amplitude. Ideally, keeping a DC link voltage 15–20

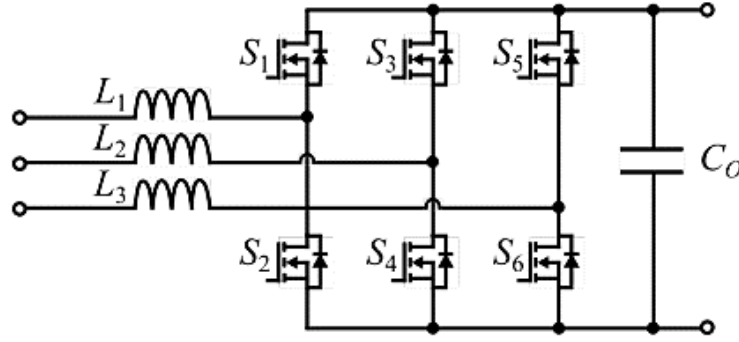


Figure 3.3: Three-phase two-level six-switch boost-type rectifier

In a two-level topology line-to-neutral rectifier, the voltage is either zero or matches the DC link voltage. Consequently, this gives rise to a three-level line-to-line voltage.

3.4 Three-Phase Three-Level Neutral Point Clamped Converter

The configuration of a three-phase three-level neutral point clamped (NPC) converter is illustrated in 3.4. Comprising twelve active switches, six diodes, and filters, this three-level topology offers advantages over the two-level converter. Notably, switches in this arrangement experience reduced voltage stress and lower switching losses, while the passive filter size is also smaller. However, the trade-off involves an increased part count, leading to potential drawbacks in system reliability, complexity, and implementation effort.

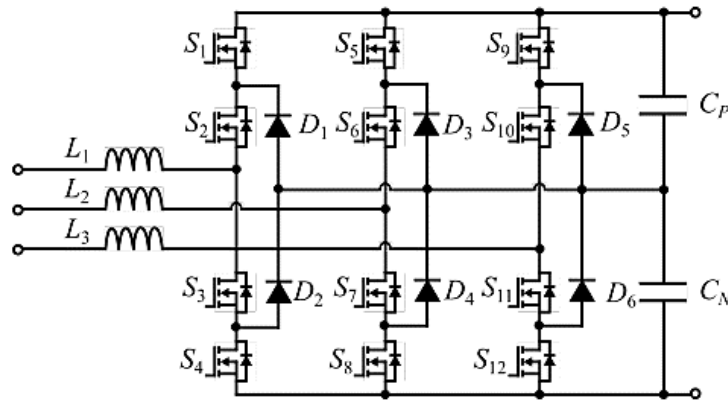


Figure 3.4: Three-phase three-level neutral point clamped converter

In a three-level topology, the line-to-neutral voltage can take values of 0.5 VDC, zero, or -0.5 VDC, resulting in a five-level line-to-line voltage. Despite the increase in complexity, the NPC converter keeps a sinusoidal grid side current similar to the two-level topology, featuring harmonics around the switching frequency and its multiples during harmonic analysis.

The primary limitation of the NPC topology lies in its use of twelve active and six passive switches, resulting in increased costs and complexity. Despite these drawbacks, it offers notable advantages such as a substantial reduction in inductor size and ensures that all switches are exposed to only half the DC link voltage. However, this configuration needs two capacitors in series, leading to higher capacitance values and lower capacitor voltage ratings.

3.5 Three-Phase Three-Level T-Type Converter

Three-phase three-level T-type converter is a bidirectional variation of the three-phase Vienna rectifier. The topology is shown in 3.5. This rectifier uses twelve active switches, compared to the original unidirectional topology that uses six diodes and six active switches. Moreover, it has three boost inductors on the AC side and a split capacitor on the DC side. This is a three-level topology similar to NPC. However, it has lower semiconductor losses for low switching frequencies compared to NPC, and it can be implemented using standard six-pack modules. This topology uses switches for two different voltage ratings.

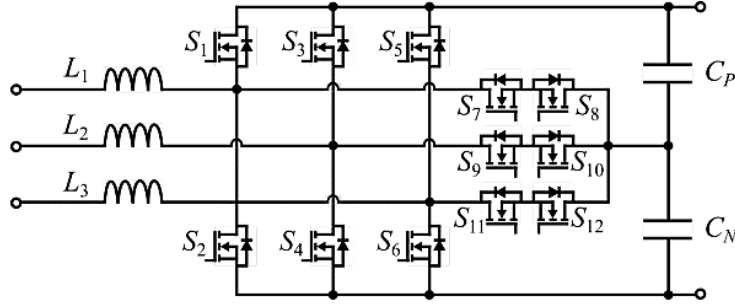


Figure 3.5: Three-phase three-level T-type converter

The three-level T-type rectifier also generates a three-level line-to-neutral voltage and five-level line-to-line voltage. The current is quite similar to the NPC converter current, also it uses similar filter sizes and filter ratings as the NPC. The main difference is the number and rating of the switches.

The two switches between positive and negative DC link block voltages between 0.5 VDC and VDC, so they must be rated for VDC. However, when these devices are switching, the voltage level changes between zero and 0.5 VDC, which results in lower switching losses compared to switching with full VDC. The devices connected between the phase leg midpoint and DC link midpoint block 0.5 VDC, so they only need to be rated for 0.5 VDC. Moreover, they also switch between zero and 0.5 VDC. Overall, the reduced number of components compared to NPC, while keeping switching from 0.5 VDC, results in higher efficiency than NPC. The efficiency of the T-type rectifier at full load is 98.95%.

Chapter 4

Implementation of Closed-Loop AC/DC Converter

We will now address challenges through the design and implementation of a closed-loop AC/DC rectifier system. The closed-loop architecture, with its feedback mechanism, promises not only enhanced control over the rectification process but also the mitigation of issues associated with traditional rectifiers. The journey towards an optimized closed-loop system involves a meticulous exploration of key components, each playing a pivotal role in achieving the desired efficiency and stability.

The aims of this research encompass a detailed examination of critical aspects, including filter selection, DC-link configuration, phase-locked loop (PLL), Clarke and Park transformations, and Proportional-Integral-Derivative (PID) control.

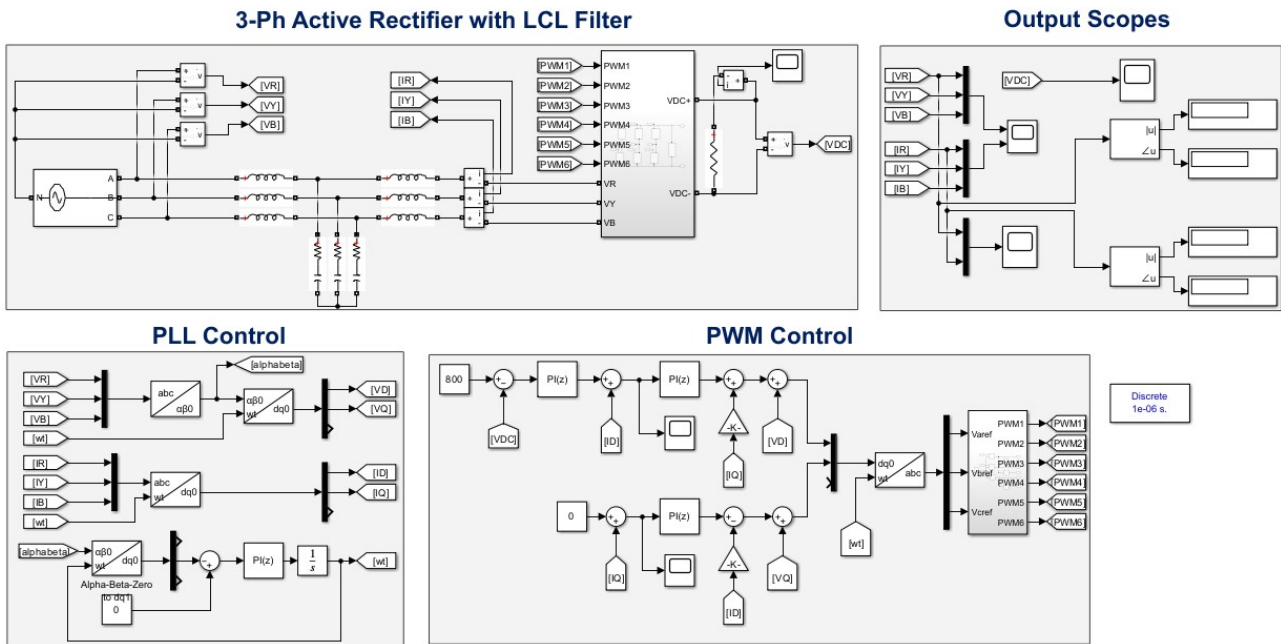


Figure 4.1: The implemented model of 10KW system using VOC

4.1 Proportional Integral Derivative (PID)

A proportional–integral–derivative controller (PID controller) is a control loop mechanism employing feedback that is widely used in industrial control systems and a variety of other applications requiring continuously modulated control. As implied by its name, the PID controller combines proportional control with added integral and derivative adjustments, helping the unit to automatically compensate for changes in a system.

Proportional-Integral-Derivative (PID) control is the most common control algorithm used in industry and has been universally accepted in industrial control. The popularity of PID controllers can be attributed partly to their robust performance in a wide range of operating conditions and partly to their functional simplicity, which allows engineers to run them in a simple, straightforward manner. The PID algorithm consists of three basic coefficients; proportional, integral, and derivative which are varied to get best response.

PID controller keeps the output such that there is zero error between process variable and set point (desired output) by closed loop operations and tuning PID parameters. PID uses three basic control behaviors.

4.1.1 P-Controller

Proportional or P- controller gives an output that is proportional to error $e(t)$. It compares the desired or set point with the actual value or feedback process value.

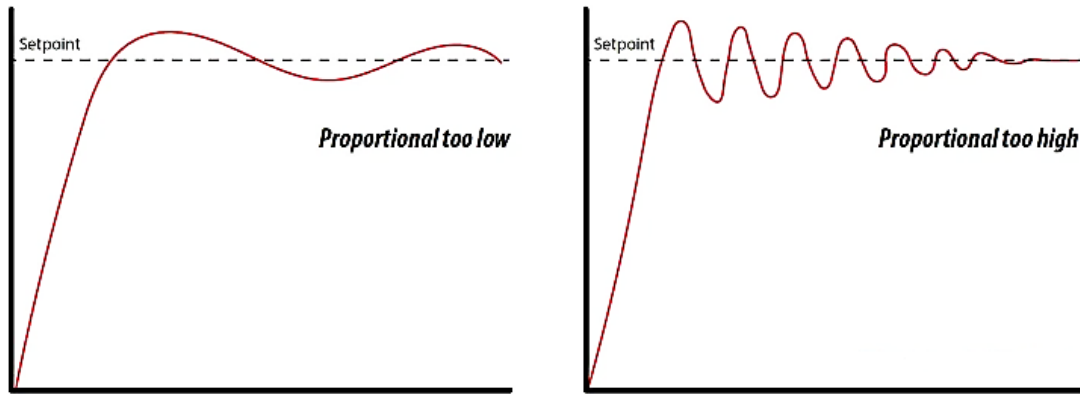


Figure 4.2: The effect of P-gain on a system

The resulting error is multiplied with a proportional constant to get the output. If the error value is zero, then this controller output is zero. This controller requires biasing or manual reset when used alone. This is because it never reaches the steady-state condition. It supplies stable operation but always keeps the steady-state error. The speed of the response is increased when the proportional constant K_P increases. P-Controller Equation:

$$u(t) = K_p e(t) \quad (4.1)$$

4.1.2 I-Controller

Due to the limitation of p-controller where there always exists an offset between the process variable and set-point, I-controller is needed, which supplies necessary action to cut the steady-state error.

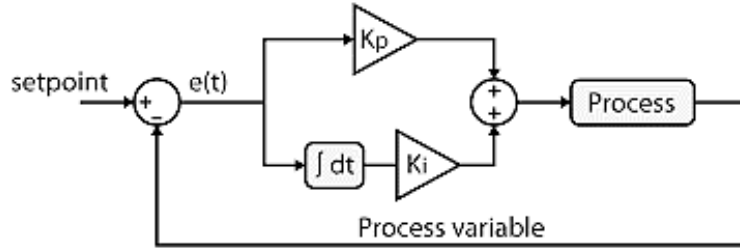


Figure 4.3: PI-control process

It integrates the error over a period of time until the error value reaches zero. It holds the value to the final control device at which the error becomes zero. Integral control decreases its output when a negative error takes place. It limits the speed of response and affects the stability of the system. The speed of the response is increased by decreasing integral gain, K_i . PI-Controller Equation:

$$u(t) = K_p e(t) + K_i \int_0^t e(\tau) d\tau \quad (4.2)$$

4.1.3 D-Controller

I-controller does not have the capability to predict the future behavior of error. So, it reacts normally once the set-point is changed. D-controller overcomes this problem by expecting the future behavior of the error. Its output depends on the rate of change of error with respect to time, multiplied by derivative constant. It gives the kick start for the output thereby increasing system response.

In 4.4, response of D, the controller is more, compared to the PI controller, and also settling time of output is decreased. It improves the stability of the system by compensating for phase lag caused by I- controller. PID Controller Equation:

$$u(t) = K_p e(t) + K_i \int_0^t e(\tau) d\tau + K_d \frac{de(t)}{dt} \quad (4.3)$$

The following figure shows the structure of the PID controller. It consists of a PID block which gives its output to the process block. Process/plant consists of final control devices like actuators, control valves, and other control devices to control various processes of industry/plant. A feedback signal from the process plant is compared with a set point or reference signal $r(t)$ and the corresponding error signal $e(t)$ is fed to the PID algorithm.

According to the proportional, integral, and derivative control calculations in the algorithm, the controller produces a combined response or controlled output which is applied to plant control devices.

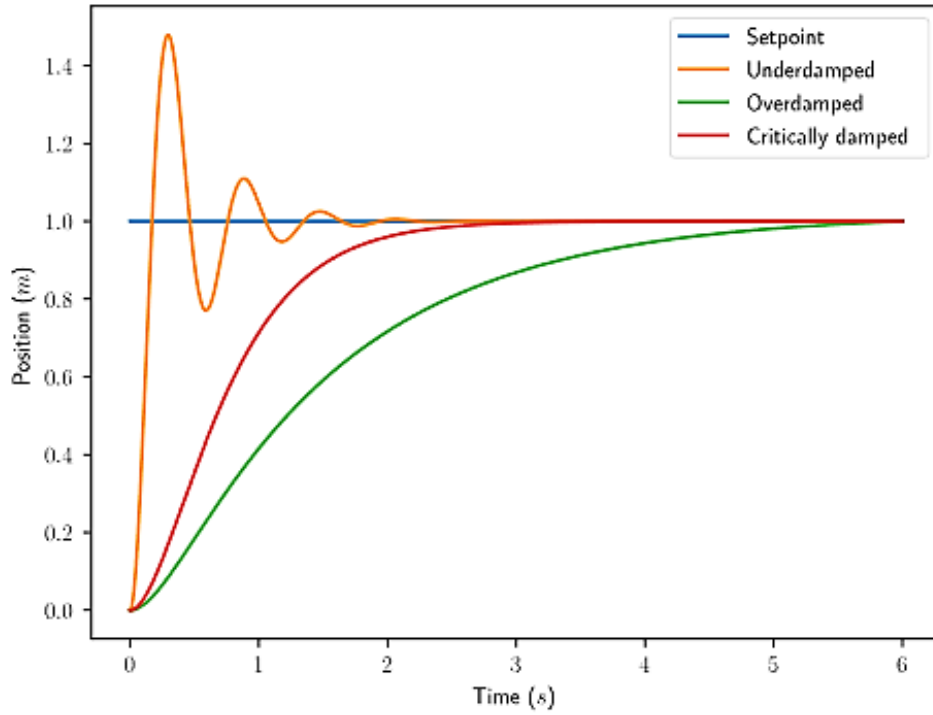


Figure 4.4: PID control on a system

4.1.4 Tuning of PID Controller

Before the working of PID controller takes place, it must be tuned to suit the dynamics of the process to be controlled. Several types of tuning methods are developed to tune the PID controllers and require much attention to select the best values of proportional, integral, and derivative gains. Some of these methods are Trial and Error method, Process reaction curve technique and Zeigler-Nichol's method. We used Trial and Error method in our project as it is simple and time effective. It is done by firstly setting k_i to zero then increasing k_p until the system reaches oscillating behavior at constant rate. Once it is oscillating, it is time to adjust k_i so that oscillations are reduced.

4.1.5 The Main Control Circuit

The following figure shows the main control circuit which is used to control the voltage with the outer loop and the current with the inner loop and finally generates the corresponding PWM signals that are used to run and control the inverter.

There are a lot of methods to control but we used a Voltage Oriented Control for its simplicity [4]. In voltage-oriented control (VOC), the line input current is oriented with respect to the line voltage vector. The line voltage vector can be obtained by measurement by using sensors or estimation. In synchronous rotating reference frame, the d-axis is aligned with the line voltage vector. The d-axis component of the line current " i_d " is proportional to the active power and its q-axis component is proportional to reactive power. To achieve unity power factor the reactive component of current reference i_q^* is set to zero. While the active component of current reference i_d^* is obtained from the PI controller, which gives the output by comparing the dc link voltage at the output with the reference

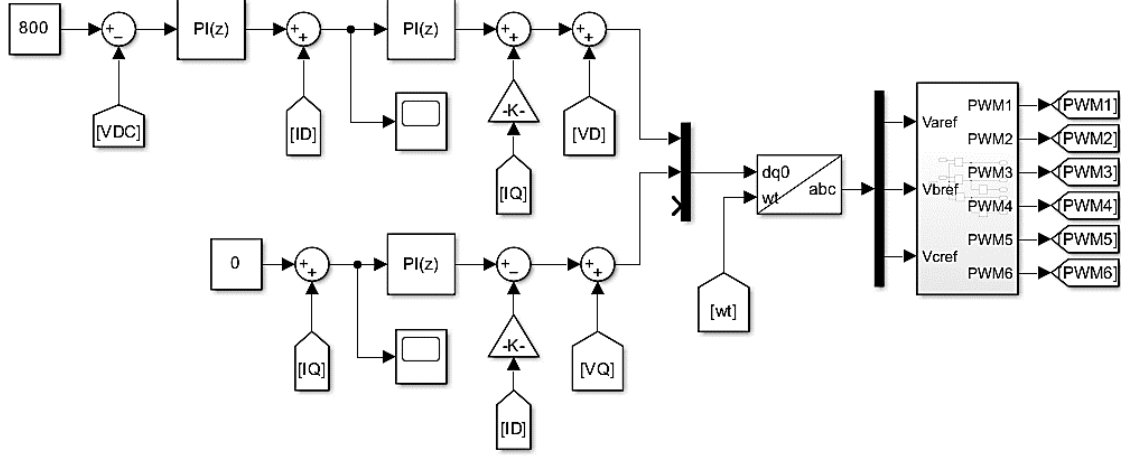


Figure 4.5: Control circuit of AFE (Active Front-end Rectifier) with 800V output voltage

voltage set as per the load requirements.

Coupling occurs due to voltage drop across inductors due to orthogonal current component coming in phase with the voltage components. Decoupling is essential to have proper control.

$$V_{sd} = V_{ld} - L \frac{di_d}{dt} + \omega L i_q \quad (4.4)$$

$$V_{sq} = V_{lq} - L \frac{di_q}{dt} - \omega L i_d \quad (4.5)$$

The voltage V_{lq} is zero by aligning the line voltage vector along the d-axis and q-axis current is regulated to zero. The current controller is decoupled as

$$V_{sd} = \omega L i_{lq} + V_{ld} + \Delta V_d \quad (4.6)$$

$$V_{sq} = -\omega L i_{ld} + \Delta V_q \quad (4.7)$$

where

$$\Delta V_d = K_p (i_d^* - i_d) + K_i \int (i_d^* - i_d) dt \quad (4.8)$$

$$\Delta V_q = K_p (i_q^* - i_q) + K_i \int (i_q^* - i_q) dt \quad (4.9)$$

In VOC it is possible to calculate the voltage across the input inductor by differentiating the current flowing through it. It is then possible to estimate the line voltage by adding voltage drop across the inductor with rectifier input voltage.

4.2 Phase-Locked Loop (PLL)

The reason why we need PLL is: suppose we want to send an active current to the grid the current should be in phase with the voltage that means that for grid connected inverters we need synchronization, so a reference signal is generated which is in phase with the actual voltage with an amplitude of 1, -1 using phase-locked loop (PLL).

The signal is used as a reference for the implementation of current controller in the grid connected inverters. There are two methods of phase locked loop implementation:

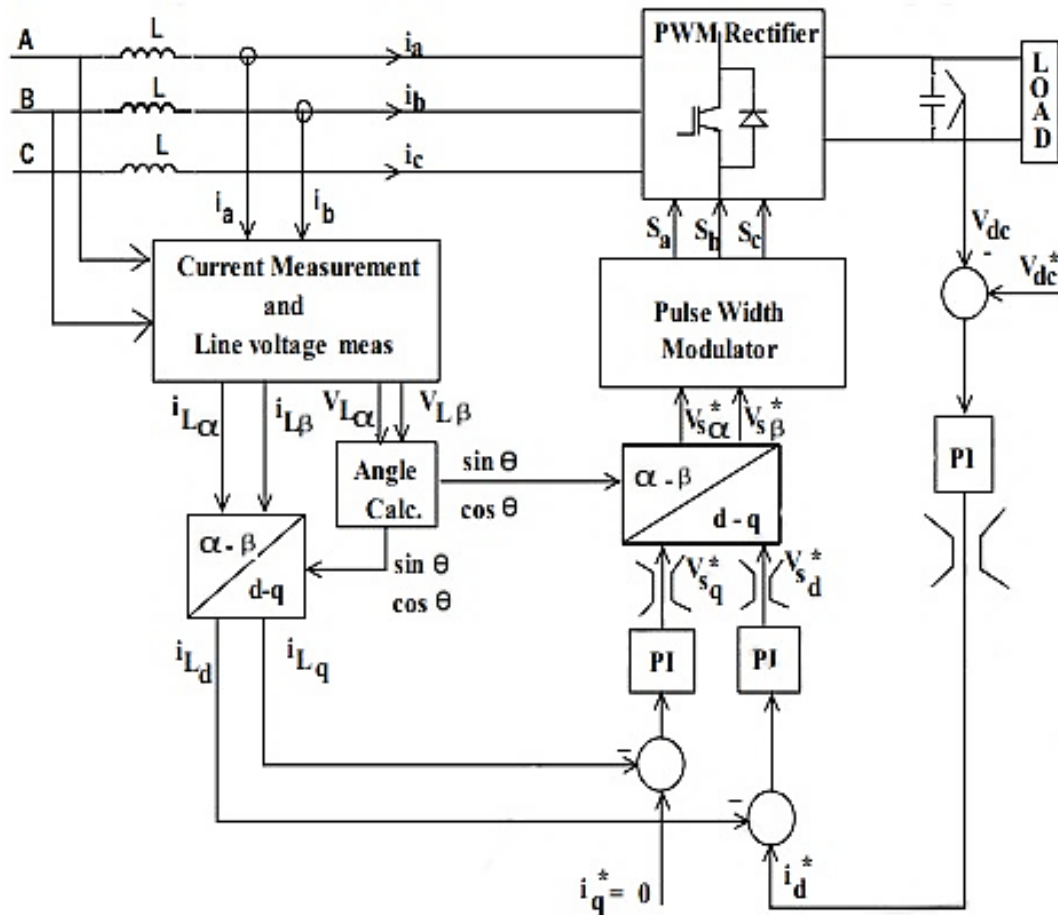
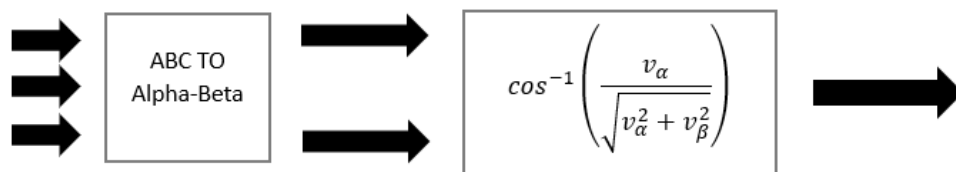


Figure 4.6: PI control loop of AFE

4.2.1 Method I

Here ABC voltages are converted into α, β voltages taking the equation shown in the diagram below giving us the angle information and from this angle information we generate reference signal but, there are few problems with this method and not used in many applications.



The problems are mainly:

- It is merely an algebraic method with simple mathematics involved.
- Open loop system so any outer effects or conditions can lead the grid to unstable condition so PLL cannot withstand harmonics, surges, noise, and spikes.
- Drift of angle and giving wrong angle information due to the mentioned effects.

But we can get rid of these problems by using closed loop phase locked loop (PLL).

4.2.2 Method II

Here we also start by transforming ABC signals into $\alpha - \beta$ signals then into dq voltages as shown in the figure below, this method is also called voltage oriented control (VOC), where the line input current is oriented with respect to the line voltage vector [5].

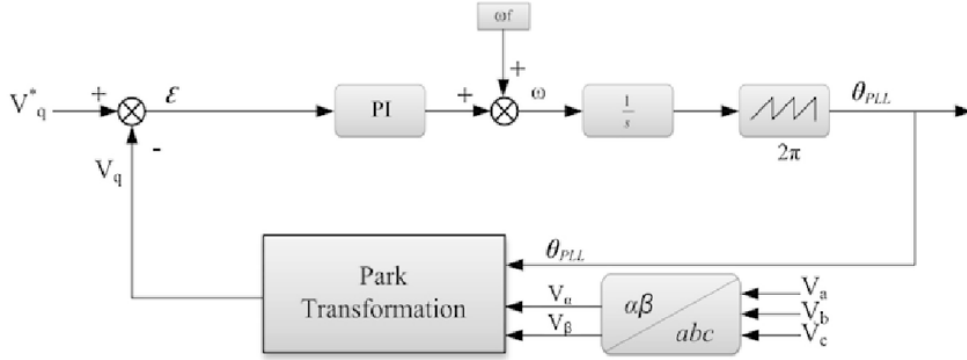


Figure 4.7: PLL control using VOC method

We can observe from the phasor diagram that D-axis is not aligned with the grid voltage so, by using the control mechanism shown in the figure we can make $V_q = 0$ using a PI controller and then the o/p is given to an integrator to find ωt .

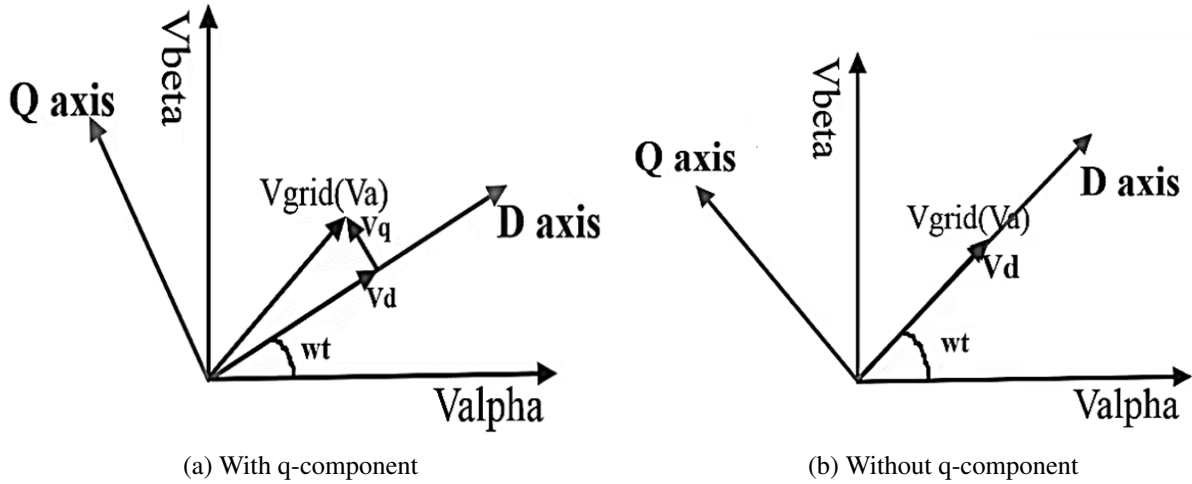


Figure 4.8: $\alpha - \beta$ signals to d-q signals

After making the V_q equal to zero the D-axis got aligned with the grid voltage and the angle between alpha-component and the D-axis has also changed to a new value which will be the angle used in generating the reference signal.

4.3 Clarke and Park Transformations

Clarke and Park transforms are commonly used in field-oriented control of three-phase AC machines. The Clarke transform converts the time domain components of a three-phase system (in ABC frame) to two components in an orthogonal stationary frame ($\alpha - \beta$). The Park transform converts the two

components in the $\alpha - \beta$ frame to an orthogonal rotating reference frame (d-q). Implementing these two transforms in a consecutive manner simplifies computations by converting AC current and voltage waveform into DC signals.

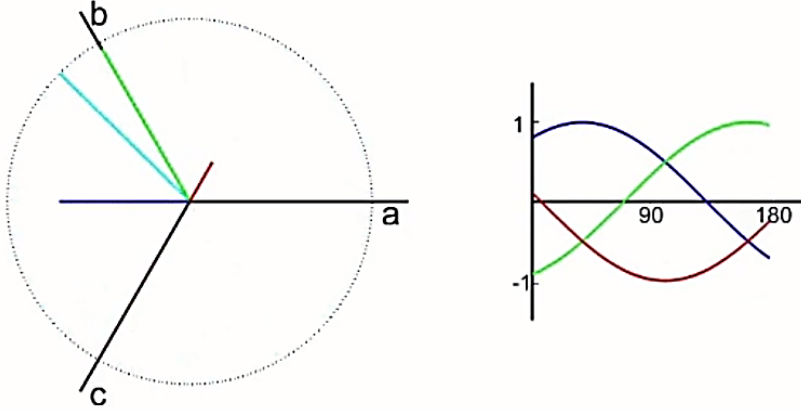


Figure 4.9: ABC frame

4.3.1 Clarke Transform

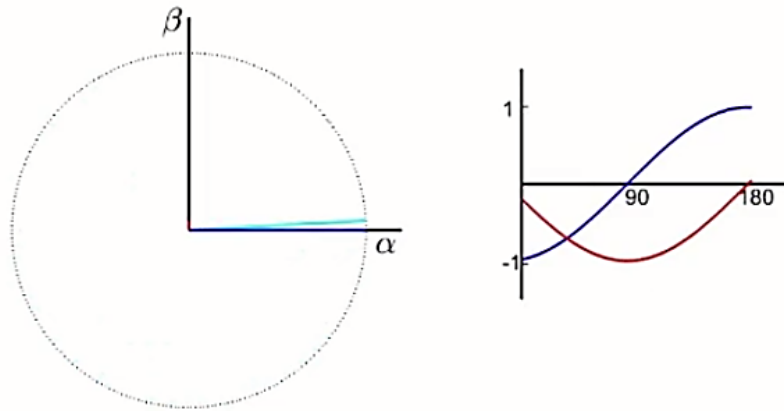


Figure 4.10: Clarke transform

The Clarke Transform converts the time-domain components of a three-phase system in an ABC reference frame to components in a stationary $\alpha\beta 0$ reference frame. For a balanced system, the zero part is equal to zero. The block implements the Clarke transform as

$$\begin{bmatrix} \alpha \\ \beta \\ 0 \end{bmatrix} = \frac{2}{3} \begin{bmatrix} 1 & \frac{-1}{2} & \frac{-1}{2} \\ 0 & \frac{\sqrt{3}}{2} & \frac{-\sqrt{3}}{2} \\ \frac{1}{2} & \frac{1}{2} & \frac{1}{2} \end{bmatrix} \begin{bmatrix} a \\ b \\ c \end{bmatrix} \quad (4.10)$$

where

- a, b, and c are the components of the three-phase system in the ABC reference frame.
- α and β are the components of the two-axis system in the stationary reference frame.
- 0 is the zero component of the two-axis system in the stationary reference frame.

4.3.2 Park Transform

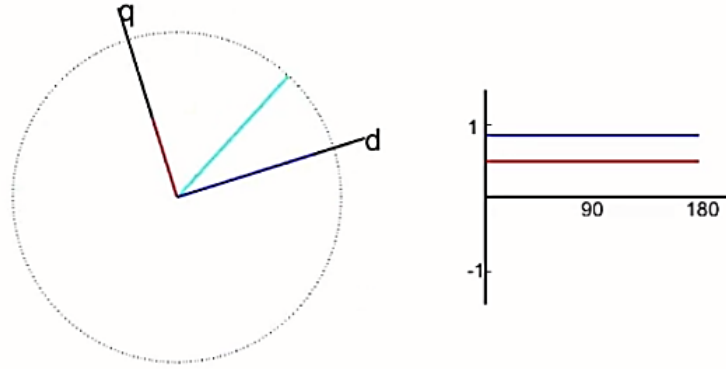


Figure 4.11: Park transform

The Park Angle Transform block converts the alpha, beta, and zero components of Clarke Transformer in a stationary reference frame to direct, quadrature, and zero components in a rotating reference frame. For balanced three-phase systems, the zero components are equal to zero.

The Clarke to Park Angle Transform block implements the transform for an a-phase to q-axis alignment as

$$\begin{bmatrix} d \\ q \\ 0 \end{bmatrix} = \begin{bmatrix} \sin(\theta) & -\cos(\theta) & 0 \\ \cos(\theta) & \sin(\theta) & 0 \\ 0 & 0 & 1 \end{bmatrix} \begin{bmatrix} \alpha \\ \beta \\ 0 \end{bmatrix} \quad (4.11)$$

where

- α and β are the components of the two-axis system in the stationary reference frame.
- 0 is the zero component of the two-axis system in the stationary reference frame.
- d and q are the direct-axis and quadrature-axis components of the two-axis system in the rotating reference frame.

4.4 Filter Design

As we are concerned about our health, we use water filters to purify the water. The same happens with electricity; there are impurities in it called harmonics, which are not wanted in our electrical systems. Harmonics affect electrical equipment, increasing its heat, reducing its lifetime and efficiency, and

introducing noise to any system connected to the grid. These are just a few of the negativities of harmonics.

So, we use filters, which are devices that filter the frequency of electronic signals by manipulating the waves' amplitude and phase shift. As we know, the sine wave has its amplitude and phase shift, so anything outside the boundaries of its amplitude and phase shift is not desired and needs to be eliminated. This leads us to Fourier series, a mathematical theory that analyzes the signal into the fundamental wave and its harmonics.

There are two types of filters: active and passive. Not all filters are suitable for every application, and not all filters remove all harmonic frequencies. Therefore, we need to carefully choose the suitable filter for each application.

4.4.1 Active Filters

They are called active because they need an external power source to operate and are built of op-amps. The main advantage of these filters is that the output signals meet low resistance, allowing the signals to be amplified, and we can also control the gain's value to control the output signal amplitude. Some common types of active filters are low-pass filters, high-pass filters, band-pass filters, and band-stop filters.

These filters are used at low frequencies, so we cannot use inductors in active filters as we know that $X_L = 2\pi fL$. At low frequencies, the reactance would be extremely low, so the low-frequency harmonics would not be eliminated; we can say that they would not be noticed by the filter. Therefore, if there is an application or system that operates at low frequencies, it is more efficient to use active filters.

4.4.2 Passive Filters

They are used in high switching frequency systems because op-amps cannot manage this range of power and frequency and grid-connected systems. We need to cut the harmonics that accompany the current out of the grid as they are called passive, so they do not need an external power source to operate. We can logically estimate why these passive filters are very well used in grid-connected systems. We need to purify the signals out from the grid, so we cannot use them to supply the active filter. Therefore, we use passive filters. There are three types of passive filters: L, LC, and LCL filters. There are also two types, one called a trap filter and the other called a notch filter, but we are not interested in these types in this paper.

L-type Filter

The simplest and most widely used passive filter is the L-type filter, consisting of a single inductor connected in series with the inverter output. It offers low-pass filtering characteristics, effectively attenuating high-frequency harmonics while allowing fundamental frequency components to pass through. However, its effectiveness is limited to lower switching frequencies and may require larger inductors for higher power applications, leading to higher costs. This leads to LC and LCL filters.

LC-type Filter

An LC-type filter incorporates both an inductor (L) and a capacitor (C) in a series-parallel configuration. It supplies enhanced filtering performance compared to the L-type filter, offering a higher attenuation rate and broader harmonic suppression. However, its disadvantage, like the L-filter, is that at high switching frequencies, we need to use bulky inductors, leading to the same cost problem as before.

LCL-type Filter

The LCL-type filter is a more advanced filter topology, featuring two inductors (L) separated by a capacitor (C). It offers superior harmonic suppression and a lower resonant frequency compared to the LC-type filter, making it suitable for higher power applications and higher switching frequencies. However, its design is more complex, and its main disadvantage is that there is some instability in frequencies near the resonant frequency. Damping resistors are added in series or parallel to the capacitor to prevent resonance-related instability.

4.4.3 Grid-Connected Inverters

The main consideration in choosing between LC and LCL filters is whether the system is connected to the grid or not. Suppose we have an inverter connected to the grid, as in Figure 4.12. We cannot use an LC filter here.

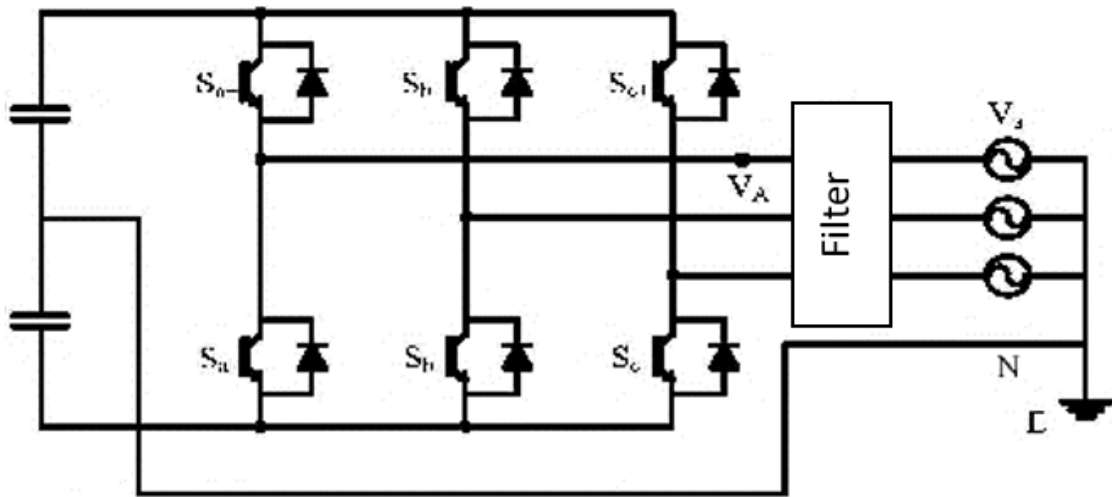


Figure 4.12: Three-phase inverter with passive filter

If we use an LC filter, the capacitors would be considered capacitive loads to the grid, so the power factor (PF) would be leading. This means that the voltage across the capacitors would come before the grid's voltage, and the output current from the inverter would not pass through to the grid but would flow to the capacitors.

In high-frequency harmonics, the grid impedance is less than the capacitive reactance, so in an LC filter, the current will flow to the grid with harmonics. However, in the case of an LCL filter,

the grid-connected inductor will block the current, and it will flow to the capacitors. Therefore, we use LCL filters in grid-connected inverters because of the tiny impedance of the grid, which causes a problem in high frequencies.

Here are some specific scenarios where an LCL filter would be a better choice than an LC filter:

- Grid-connected inverters: LCL filters are commonly used in grid-connected inverters to attenuate harmonics and follow grid harmonics standards. The lower resonant frequency of LCL filters makes them less susceptible to resonances caused by the grid impedance.
- High-power applications: In high-power applications, the switching frequency of the power converter is often higher to reduce the size and weight of the inductors and capacitors. This higher switching frequency can lead to more harmonics, so an LCL filter is often necessary to supply adequate attenuation.
- Applications with a sensitive load: If the load is sensitive to harmonics, such as a motor or a computer system, an LCL filter can help to protect the load from damage.

4.4.4 Method I

This method discusses the empirical design of L filter. Note that this method is not based on any reference but practical experience in the field. L filter was extremely popular until IEEE 519- 1992 standards were introduced. Because to meet all the requirements in the standards, the L filter rating and size become remarkably high.

The following parameters are needed for the design: E_n – Line to line RMS voltage (rectifier input), f_g – grid frequency and S_{rated} – apparent rated power. The base impedance is calculated using equation 4.12

$$Z_b = \frac{E_n^2}{S_{rated}} \quad (4.12)$$

We can assume that the inductive reactance (X_L) is roughly around 5% to 10% of the base impedance. Thus, we can calculate the inductive reactance and the inductance using the following equations:

$$X_L = (0.05 \text{ to } 0.1)Z_b \quad (4.13)$$

where

$$L = \frac{X_L}{2\pi f_g} \quad (4.14)$$

The addition of a resistor in series with the inductor in an L filter is crucial for maintaining stability, protecting components, and complying with EMI standards in grid-connected inverter applications. This resistor value can be empirically calculated as third of the inductive reactance as shown in the following equation:

$$R = \frac{X_L}{3} \quad (4.15)$$

Design Example

A step-by-step procedure to obtain parameters of the filter with considering the following given data, needed for the filter design: $E_n = 380\text{V}$ - line to line RMS voltage, $P_{rated} = 1000\text{W}$ - rated active power,

$f_g = 50\text{Hz}$ -grid frequency.

Considering a unity power factor system:

$$S_{rated} = P_{rated} = 1000VA$$

Therefore, the base impedance and the base capacitance are:

$$Z_b = \frac{380^2}{1000} = 144.4\Omega$$

The filter inductive reactance can be calculated by:

$$X_L = 0.1 * 144.4 = 14.4\Omega$$

To calculate the inductance:

$$L = \frac{14.4}{2\pi * 50} = 45mH$$

Therefore, the resonant frequency satisfies the equation, and the damping resistance can be calculated as follows:

$$R = \frac{14.4}{3} = 4.8\Omega$$

Simulation

A simulation of method I was done on MATLAB-Simulink to check the performance of the system with the filter using the design example that was mentioned previously in that method. Here is the output voltage V_{DC} :

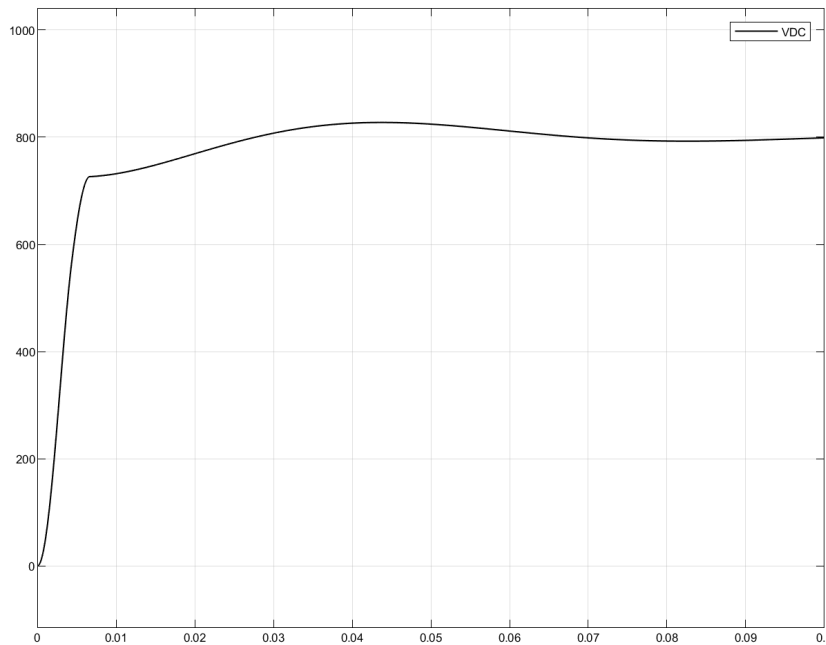


Figure 4.13: The output voltage on the DC-link – method I

Also, we had to check the phase shift between voltage and current of one of the phases as shown in Figure 4.14:

Note that this is not the actual waveform of the current but a multiple of it. It was multiplied by fifty just so we can observe the two wave-forms at the same time.

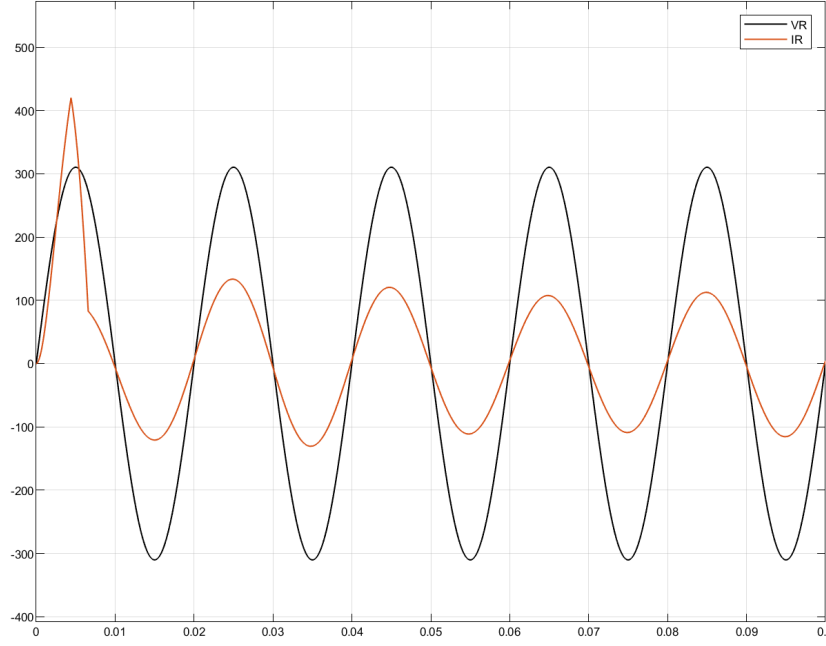


Figure 4.14: The current and the phase voltage of phase R – method I

4.4.5 Method II

The design of LCL filters must consider several critical constraints, including current ripple, filter size, and switching ripple attenuation. As noted in [6], the reactive power variation introduced by the capacitor can cause resonance, potentially destabilizing the system. To address this issue, a damping mechanism, such as a resistor in series with the capacitor, is recommended.

This method meticulously outlines the LCL filter design process, emphasizing the importance of proper damping to prevent resonance. The algorithm for selecting LCL filter parameters utilizes the converter's power rating, grid frequency, and switching frequency as inputs.

The following parameters are needed for the design: E_n – Line to line RMS voltage (rectifier input), V_{ph} – phase voltage (rectifier input), P_n – rated active power, V_{DC} – DC bus voltage, f_g – grid frequency, f_{sw} – switching frequency and f_{res} – resonance frequency.

The base impedance and base capacitance are defined by equations 4.16 and 4.17. Thus, the filter values will be referred in % of the base values:

$$Z_b = \frac{E_n^2}{P_n} \quad (4.16)$$

$$C_b = \frac{1}{\omega_n Z_b} \quad (4.17)$$

For the design of the filter capacitance, it is considered that the maximum power factor variation seen by the grid is 5%, as it is multiplied by the value of base impedance of the system: $C_f = 0.05C_b$, where L_i is inverter side inductor. A 10% ripple of the rated current for the design parameters is given by:

$$\Delta I_{Lmax} = 0.1 I_{max} \quad (4.18)$$

where

$$I_{max} = \frac{P_n \sqrt{2}}{3V_{ph}} \quad (4.19)$$

$$L_i = \frac{V_{DC}}{6f_{sw}\Delta I_{Lmax}} \quad (4.20)$$

The main objective of the LCL filter design is in fact to reduce the expected 10% current ripple limit to 20% of its own value, resulting in a ripple value of 2% of the output current. To calculate the ripple reduction, the LCL filter equivalent circuit is first analyzed considering the inverter as a current source for each harmonic frequency.

The following equations give the relation between the harmonic current generated by the inverter and the once injected in the grid:

$$L_g = \frac{\sqrt{\frac{1}{K_a^2} + 1}}{C_f \omega_{sw}^2} \quad (4.21)$$

where, K_a is the desired attenuation.

A resistor in series (R_f) with the capacitor attenuates part of the ripple on the switching frequency to avoid the resonance. The value of this resistor should be one third of the impedance of the filter capacitor at the resonant frequency and the resistor in series with the filter capacitance is given by 4.24.

$$\omega_{res} = \sqrt{\frac{L_i + L_g}{L_i L_g C_f}} \quad (4.22)$$

$$10f_g < f_{res} < 0.5f_{sw} \quad (4.23)$$

It is necessary to check resonant frequency to satisfy 4.23. If it does not, the parameters should be re-chosen.

$$R_f = \frac{1}{3\omega_{res}C_f} \quad (4.24)$$

Design Example

A step-by-step procedure to obtain parameters of the filter with considering the following given data, needed for the filter design: $E_n = 380V$ - line to line RMS voltage, $V_{ph} = 220V$ - phase RMS voltage, $P_n = 1000W$ - rated active power, $V_{DC} = 800V$ - DC bus voltage, $f_g = 50Hz$ -grid frequency, $f_{sw} = 10KHz$ - switching frequency, $K_a = 20\%$ - attenuation factor is done.

Therefore, the base impedance and the base capacitance are:

$$Z_b = \frac{380^2}{1000} = 144.4\Omega$$

$$C_b = \frac{1}{2\pi * 50 * 144.4} = 22\mu F$$

The filter capacitance can be calculated by:

$$C_f = 0.05 * 22 * 10^{-6} = 1.1\mu F$$

To calculate the inverter-side inductor:

$$I_{max} = \frac{1000\sqrt{2}}{3 * 220} = 2.14A$$

$$\Delta I_{Lmax} = 0.1 * 2.14 = 0.214A$$

$$L_i = \frac{800}{6 * 10000 * 0.214} = 62.3mH$$

For the grid-side inductor:

$$L_g = \frac{\sqrt{\frac{1}{0.2^2} + 1}}{1.1 * 10^{-6} (2\pi * 10000)^2} = 1.38mH$$

Now, we shall check if the system is within the stable region to avoid resonance:

$$\omega_{res} = \sqrt{\frac{1.38 * 10^{-3} + 62.3 * 10^{-3}}{1.38 * 10^{-3} * 62.3 * 10^{-3} * 1.1 * 10^{-6}}} = 25949rad$$

$$f_{res} = \frac{25949}{2\pi} = 4129.92Hz$$

$$10 * 50 < f_{res} < 0.5 * 10000$$

Therefore, the resonant frequency satisfies the equation, and the damping resistance can be calculated as follows:

$$R_f = \frac{1}{3 * 2\pi * 4129.92 * 1.1 * 10^{-6}} = 11.68\Omega$$

Simulation

A simulation of method II was done on MATLAB-Simulink to check the performance of the system with the filter using the design example that was mentioned previously in that method. Here is the output voltage V_{DC} :

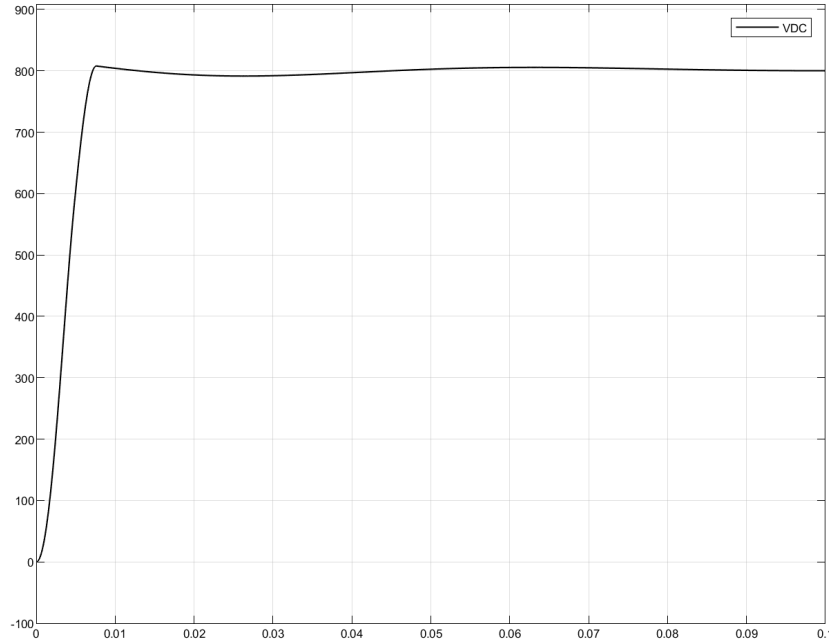


Figure 4.15: The output voltage on the DC-link – method II

Also, we had to check the phase shift between voltage and current of one of the phases as shown in Figure 4.16:

Note that this is not the actual waveform of the current but a multiple of it. It was multiplied by fifty just so we can observe the two wave-forms at the same time.

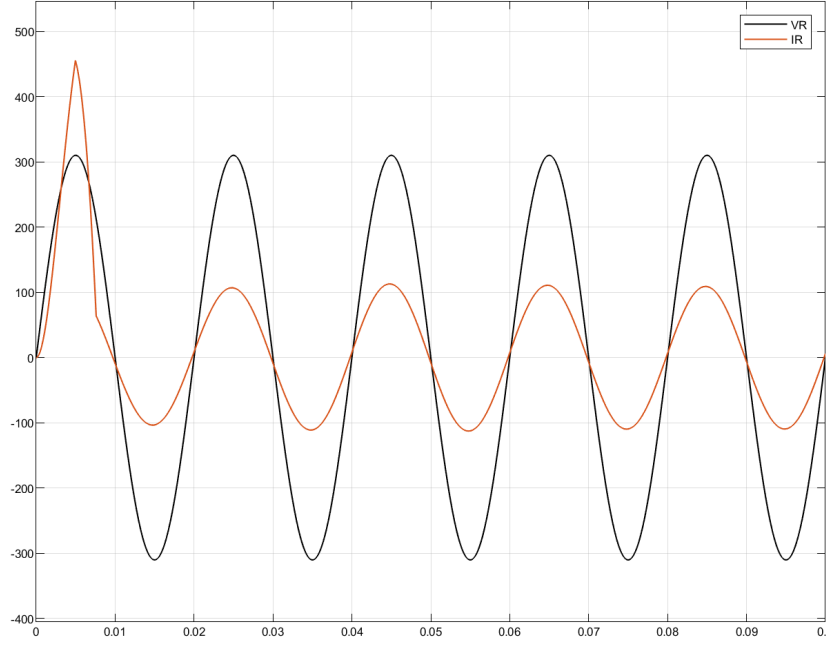


Figure 4.16: The current and the phase voltage of phase R – method II

4.4.6 Method III

The design of LCL filters plays a crucial role in grid-connected inverter applications, ensuring efficient power transfer and minimizing harmonic distortion. This method, inspired by [7], provides a comprehensive framework for designing LCL filters that meet specific performance requirements while addressing potential stability issues. The method delves into the fundamental principles of LCL filter dynamics, enabling designers to make informed decisions about filter parameter selection.

To design the filter using this method, some parameters must be provided which are: S_{rated} – apparent rated power, V_{ph} – phase voltage (rectifier input), f_g – grid frequency and f_{sw} – switching frequency.

The filter capacitance is calculated at reactive power equals 5% of the rated apparent power of the system. The reactive power is calculated as follows:

$$Q_{rated} = C_f \omega_n V_{ph}^2 \quad (4.25)$$

where ω_n is the grid angular frequency. Therefore, the filter capacitance can be calculated according to equation 4.26.

$$C_f = \frac{0.05 S_{rated}}{2\pi f_g V_{ph}^2} \quad (4.26)$$

It is worth mentioning that the resonance frequency can be calculated as in the following equation:

$$f_{res} = \frac{f_{sw}}{10} \quad (4.27)$$

The value of the inverter-side inductor is selected based on the switching current. According to IEEE, the switching current is only 0.3% of the rated grid current.

$$I_{sw} = 0.003 I_{grid} \quad (4.28)$$

where

$$I_{grid} = \frac{S_{rated}}{3V_{ph}} \quad (4.29)$$

Now, for a triangular PWM scheme, minimum value of the switching voltage at switching frequency is 90% of the grid phase voltage as shown in equation 4.30.

$$V_{sw} = 0.9V_{ph} \quad (4.30)$$

Using the equations above inductance can be calculated as:

$$L_{min} = \frac{1}{|\omega_{sw} \frac{I_{sw}}{V_{sw}} \left(1 - \frac{\omega_{sw}^2}{\omega_{res}^2}\right)|} \quad (4.31)$$

Inverter-side inductor and grid-side inductor can be assumed to have the same value which is half of the calculated inductance (L_{min}).

$$L_g = L_i = \frac{L_{min}}{2} \quad (4.32)$$

These are the minimum values of the required inductances. The maximum values are calculated based on the voltage drop across it. Voltage drop is always limited to 20% of the grid phase voltage. So maximum inductance is given by:

$$L_{max} = \frac{0.2 V_{ph}}{2\pi f_g I_{grid}} \quad (4.33)$$

Design Example

To derive the parameters essential for filter design, follow these step-by-step procedures using the provided data: $V_{ph} = 220V$ - phase RMS voltage, $P_{rated} = 1000W$ - rated active power, $f_g = 50Hz$ -grid frequency, $f_{sw} = 10KHz$ - switching frequency.

Therefore, rated apparent power can be calculated as follow:

$$S_{rated}^2 = (0.05S_{rated})^2 + 1000^2$$

$$S_{rated} \cong 1000VA$$

To calculate the filter capacitance:

$$C_f = \frac{0.05 * \left(\frac{1000}{3}\right)}{2\pi * 50 * 220^2} = 1.1\mu F$$

The resonance frequency is achieved by:

$$f_{res} = \frac{10000}{10} = 1000Hz$$

Calculating the minimum value of the inductance:

$$I_{grid} = \frac{1000}{3 * 220} = 1.51A$$

$$I_{sw} = 0.003 * 1.51 = 4.45mA$$

$$V_{sw} = 0.9 * 220 = 198V$$

$$L_{\min} = \frac{1}{|(2\pi * 10000)^{\frac{4.45*10^{-3}}{198}} \left(1 - \frac{(2\pi*10000)^2}{(2\pi*1000)^2}\right)|} = 7.15mH$$

So, the minimum value of the inverter-side and grid-side inductors is equal to:

$$L_g = L_i = \frac{7.15 * 10^{-3}}{2} = 3.58mH$$

To get the maximum value of the inductance:

$$L_{\max} = \frac{0.2 * 220}{2\pi * 50 * 1.51} = 92.75mH$$

The maximum value of the inverter-side and grid-side inductors is:

$$L_g = L_i = \frac{92.75 * 10^{-3}}{2} = 46.37mH$$

Simulation

A simulation of method III was done on MATLAB-Simulink to check the performance of the system with the filter using the design example that was mentioned previously in that method. Here is the output voltage V_{DC} :

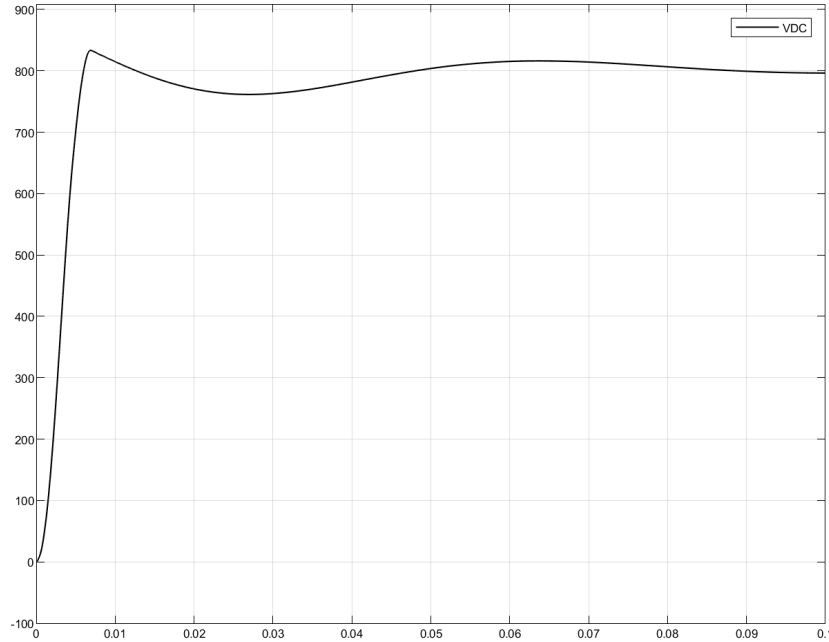


Figure 4.17: The output voltage on the DC-link – method III

Also, we had to check the phase shift between voltage and current of one of the phases as shown in Figure 4.18:

Note that this is not the actual waveform of the current but a multiple of it. It was multiplied by fifty just so we can observe the two wave-forms at the same time.

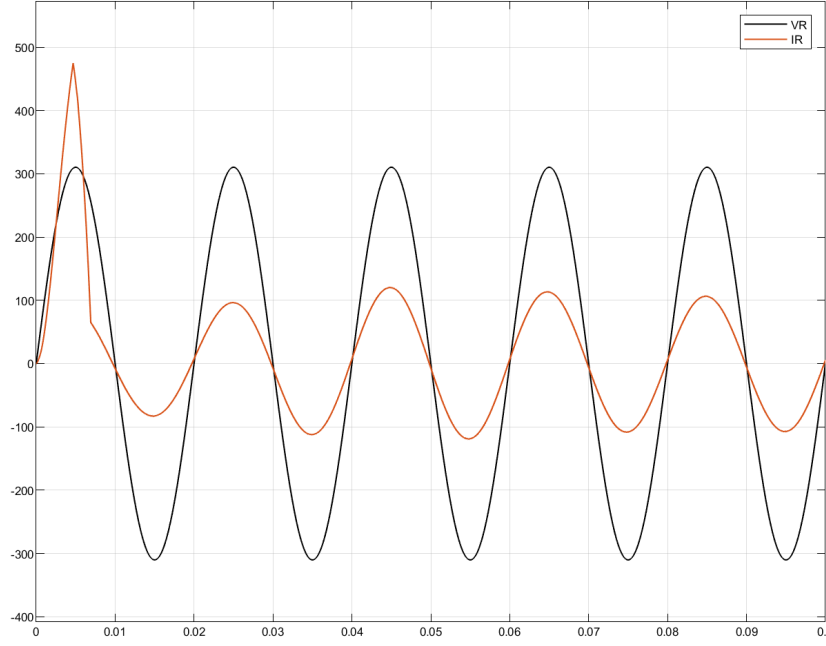


Figure 4.18: The current and the phase voltage of phase R – method III

4.4.7 Method IV

This method according to [8] deals with a design method of LCL filter for grid-connected three-phase inverters. By analyzing total harmonic distortion of the current (THD_i) in the inverter-side inductor and the ripple attenuation factor of the current (RAF) injected to the grid through the LCL network, the parameter of LCL can be clearly designed.

The base impedance of the system must be known before choosing the LCL filter parameters. The base values of the impedance, inductance, and capacitance are defined as in equations 4.34 ~ 4.36.

$$Z_b = \frac{E_n^2}{P_n} \quad (4.34)$$

$$L_b = \frac{Z_b}{\omega_n} \quad (4.35)$$

$$C_b = \frac{1}{\omega_n Z_b} \quad (4.36)$$

The inductance of inverter-side inductor is obtained by setting THD_i within 10% to 30%. If THD_i is set below 10%, the inductance is increased, and the resonant frequency decreases. If THD_i is increased more than 30%, the resonant frequency increases. The resonant frequency should be set between the bandwidth of the controller and switching frequency.

$$L_i = \frac{f_g}{f_{sw}} \times \frac{L_b}{THD_i} \times \sqrt{\frac{\pi^2}{18} \times \left(\frac{3}{2} - \frac{4\sqrt{3}}{\pi} m_a + \frac{9}{8} m_a^2 \right)} \quad (4.37)$$

where m_a is the modulation index.

$$m_a = \frac{V_{ph} 2\sqrt{2}}{V_{DC}} \quad (4.38)$$

Filter capacitance must be set properly by setting x less than 5% of base capacitance as follows:

$$C_f \leq x \frac{1}{\omega_n Z_b} \quad (4.39)$$

Use equation 4.40 to extract the grid-side inductance. After setting proper RAF, calculate the grid-side inductance.

$$L_g = \frac{RAF + 1}{RAFC_f \omega_{sw}^2} \quad (4.40)$$

Make sure the total inductance of inductor which is sum of the inductance of inverter-side inductor and grid-side inductor is less than 10% of the base value of the inductance.

Design Example

A step-by-step procedure to obtain parameters of the filter with considering the following given data, needed for the filter design: $E_n = 380V$ - line to line RMS voltage, $V_{ph} = 220V$ - phase RMS voltage, $P_n = 1000W$ - rated active power, $V_{DC} = 800V$ - DC bus voltage, $f_g = 50Hz$ -grid frequency, $f_{sw} = 10KHz$ - switching frequency, $THD_i = 20\%$ - total harmonic distortion of the current, $RAF = 20\%$ - attenuation factor is done.

Therefore, the base impedance and the base capacitance are:

$$\begin{aligned} Z_b &= \frac{380^2}{1000} = 144.4\Omega \\ L_b &= \frac{144.4}{2\pi * 50} = 0.4596H \\ C_b &= \frac{1}{2\pi * 50 * 144.4} = 22\mu F \end{aligned}$$

The filter capacitance can be calculated by:

$$C_f \leq 0.05 * 22 * 10^{-6} = 1.1\mu F$$

The modulation index is as follows:

$$m_a = \frac{220 * 2\sqrt{2}}{800} = 0.778$$

To calculate the inverter-side inductor:

$$L_i = \frac{50}{10000} \times \frac{0.4596}{0.2} \times \sqrt{\frac{\pi^2}{18} \times \left(\frac{3}{2} - \frac{4\sqrt{3}}{\pi} * 0.778 + \frac{9}{8}(0.778)^2 \right)} = 5.8mH$$

For the grid-side inductor:

$$L_g = \frac{0.2 + 1}{0.2 * 1.1 * 10^{-6} (2\pi * 10000)^2} = 1.38mH$$

To make sure the design is correct:

$$\begin{aligned} L_g + L_i &< 0.1L_b \\ 1.38 * 10^{-3} + 5.8 * 10^{-3} &< 0.1 * 0.4596 \end{aligned}$$

Therefore, the filter is well designed.

Simulation

A simulation of method IV was done on MATLAB-Simulink to check the performance of the system with the filter using the design example that was mentioned previously in that method. Here is the output voltage V_{DC} :

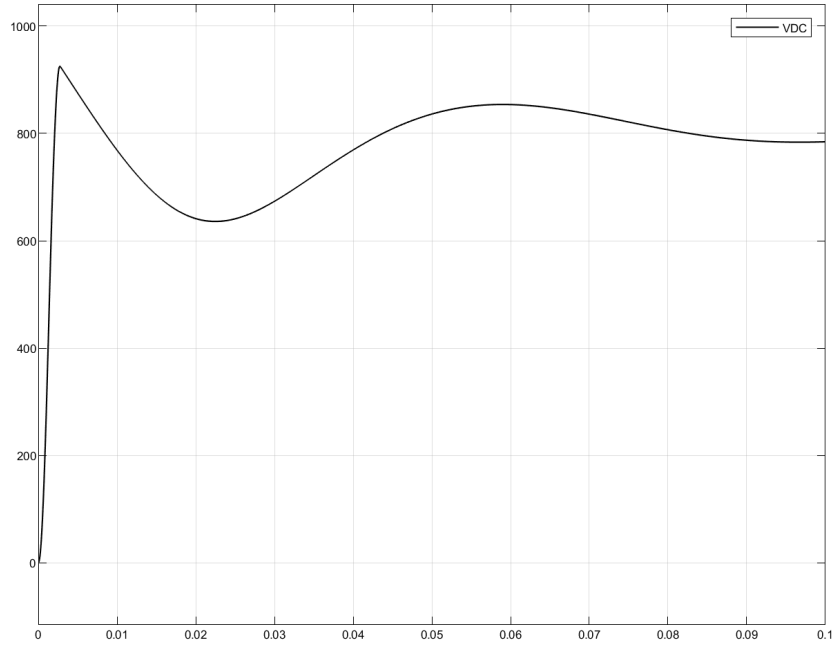


Figure 4.19: The output voltage on the DC-link – method IV

Also, we had to check the phase shift between voltage and current of one of the phases as shown in Figure 4.20:

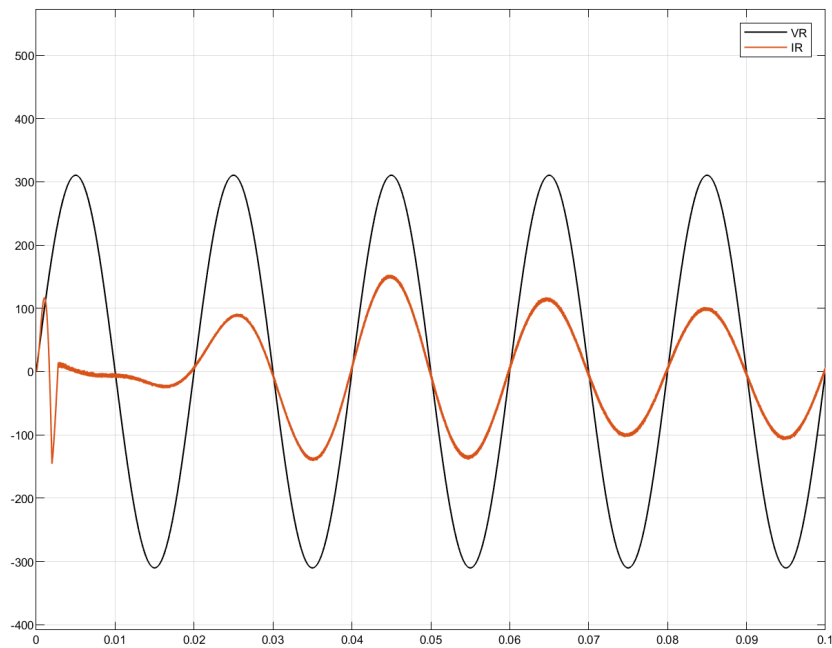


Figure 4.20: The current and the phase voltage of phase R – method IV

Note that this is not the actual waveform of the current but a multiple of it. It was multiplied by fifty just so we can observe the two wave-forms at the same time.

4.4.8 Method V

The design of LCL filter can also be done via MATLAB code that was mentioned in [9]. You may enter the system inputs like: P_n – active rated power, V_{ph} – phase voltage (rectifier input), V_{DC} – DC bus voltage, f_n – grid frequency and f_{sw} – switching frequency.

It is worth mentioning that the code that is present in [9] is for a single-phase grid-connected inverter but some of the data was changed to suit the three-phase grid-connected inverter, which is our case.

Design Example

To derive the parameters essential for filter design, follow these step-by-step procedures using the provided data: $V_{ph} = 220V$ - phase RMS voltage, $P_{rated} = 1000W$ - rated active power, $f_g = 50Hz$ -grid frequency, $f_{sw} = 10KHz$ - switching frequency, $r = 0.6$.

Therefore, the MATLAB code is as follows:

```
% System parameters
Pn = 1000; % Inverter power
Vph = 220; %Grid phase RMS voltage
Vdc=800; %DC link voltage
fn = 50; %Grid frequency
fsw = 10000; %Switching frequency

En = Vph*sqrt(3);
wn = 2*pi*fn;
ws = 2*pi*fsw;

% Base values
Zb = (En^2)/Pn
Cb = 1/(wn*Zb)

% Filter parameters
delta_Imax=0.1*((Pn*sqrt(2))/(3*Vph))
Li=Vdc/(8*fsw*delta_Imax) %Inverter side inductance
x = 0.05;
Cf = x*Cb %Filter capacitor

% Calculation of r, between Linv and Lg
r = 0.6;

% Grid side inductance
Lg = r*Li
```

```
% Calculation of frequency of the filter
wres = sqrt((Li+Lg)/(Li*Lg*Cf));
fres=wres/(2*pi)
```

```
%Damping resistance
Rd = 1/(3*wres*Cf)
```

And the LCL filter parameters as the output values of the code are as follow:

$$C_f = 1.1\mu F$$

$$L_i = 46.7mH$$

$$L_g = 28mH$$

$$R_f = 42.11\Omega$$

Simulation

A simulation of method V was done on MATLAB-Simulink to check the performance of the system with the filter using the design example that was mentioned previously in that method. Here is the output voltage V_{DC} :

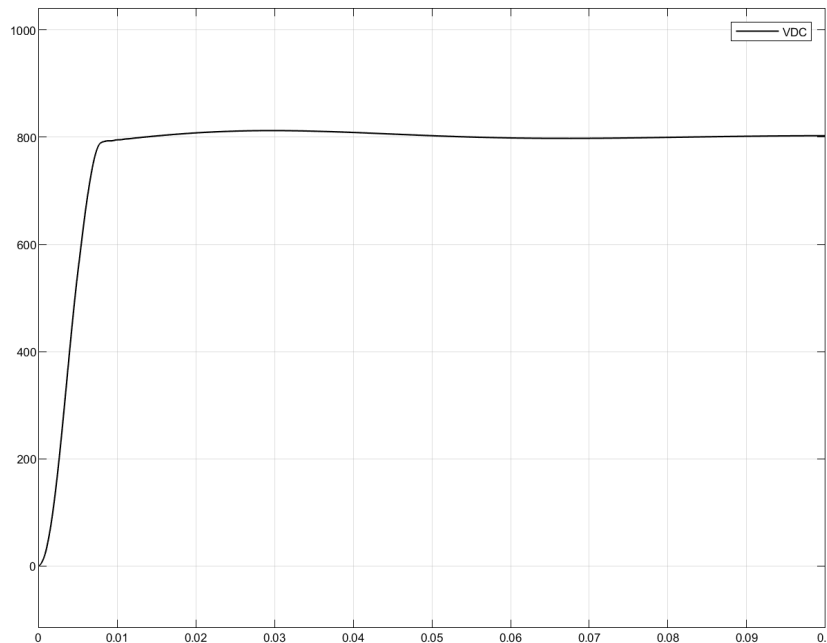


Figure 4.21: The output voltage on the DC-link – method V

Also, we had to check the phase shift between voltage and current of one of the phases as shown in Figure 4.22:

Note that this is not the actual waveform of the current but a multiple of it. It was multiplied by fifty just so we can observe the two wave-forms at the same time.

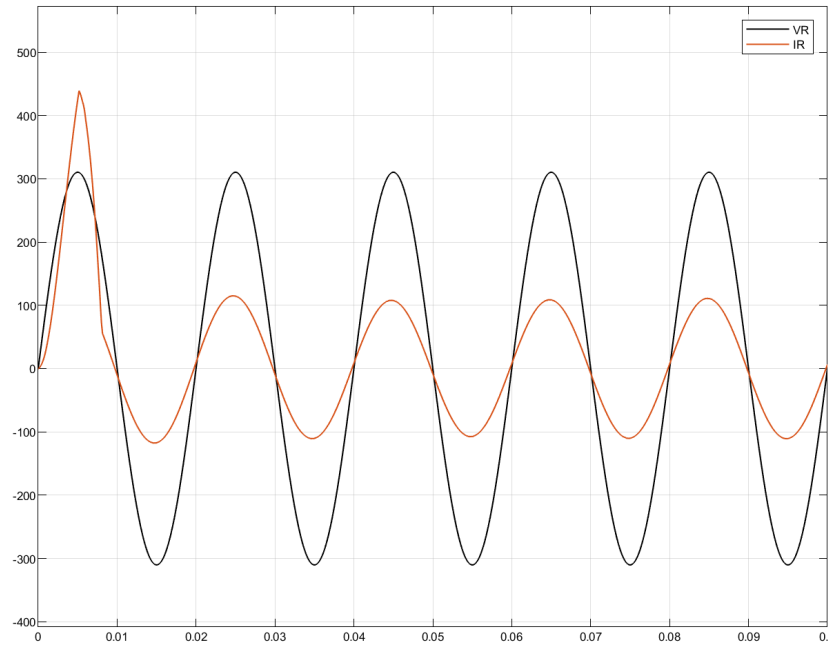


Figure 4.22: The current and the phase voltage of phase R – method V

4.4.9 Comparison

After discussing multiple methods, it is now time to compare the output of each method. The following table contains the output of each method.

<i>Method</i>	L_i (mH)	L_g (mH)	C_f (μ F)
Method I	45	-	-
Method II	62.3	1.38	1.1
Method III	3.58 – 46.37	3.58 – 46.37	1.1
Method IV	5.8	1.38	1.1
Method V	46.7	28	1.1

Table 4.1: Comparison between the output of different design methods

After learning all the different methods, each method shall be considered carefully to get the optimum output for the desired system. In our case, we have done multiple simulations to notice the output of each method. It was observed that each method produced the same output with slight differences.

Yet, Method IV had the worst output as the phase current was full of ripples even by substituting by different values of inductance within the calculated range, also the output voltage had the highest settling time.

Method II and method V had the lowest overshoot compared to the rest in this specific case, but method V had a smoother output. But at higher power (10k watt), method II had a way better response than method V leading it to be our preferred method. The PI controllers were calibrated in a way to have a leading power factor of 0.9998 with settling time of less than a half cycle with settling error of 0.5%. Also, the second method's design was checked by equation 4.23, to make sure that the design would avoid resonance problems.

4.4.10 Chosen Method

Two designs were done based on method II for both the low-rating system (1kW) and the high-rating system (10kW) to check its output.

Design Example - Low Power

A step-by-step procedure to obtain parameters of the filter with considering the following given data, needed for the filter design: $E_n = 100V$ - line to line RMS voltage, $V_{ph} = 57.73V$ - phase RMS voltage, $P_n = 1000W$ - rated active power, $V_{DC} = 200V$ - DC bus voltage, $f_g = 50Hz$ -grid frequency, $f_{sw} = 10KHz$ - switching frequency, $K_a = 20\%$ - attenuation factor is done.

Therefore, the base impedance and the base capacitance are:

$$Z_b = \frac{100^2}{1000} = 10\Omega$$

$$C_b = \frac{1}{2\pi * 50 * 10} = 3.18 * 10^{-4}F$$

The filter capacitance can be calculated by:

$$C_f = 0.05 * 3.18 * 10^{-4} = 15.915\mu F$$

To calculate the inverter-side inductor:

$$I_{max} = \frac{1000\sqrt{2}}{3 * 57.73} = 8.16A$$

$$\Delta I_{Lmax} = 0.1 * 8.16 = 0.816A$$

$$L_i = \frac{200}{6 * 10000 * 0.816} = 4mH$$

For the grid-side inductor:

$$L_g = \frac{\sqrt{\frac{1}{0.2^2} + 1}}{15.915 * 10^{-6} (2\pi * 10000)^2} = 95.492\mu H$$

Now, we shall check if the system is within the stable region to avoid resonance:

$$\omega_{res} = \sqrt{\frac{4 * 10^{-3} + 95 * 10^{-6}}{4 * 10^{-3} * 95 * 10^{-6} * 15.915 * 10^{-6}}} = 25952.26rad$$

$$f_{res} = \frac{25952.26}{2\pi} = 4130.4Hz$$

$$10 * 50 < f_{res} < 0.5 * 10000$$

Therefore, the resonant frequency satisfies the equation, and the damping resistance can be calculated as follows:

$$R_f = \frac{1}{3 * 2\pi * 4130.4 * 16 * 10^{-6}} = 0.8027\Omega$$

Design Example - High Power

A step-by-step procedure to obtain parameters of the filter with considering the following given data, needed for the filter design: $E_n = 380V$ - line to line RMS voltage, $V_{ph} = 220V$ - phase RMS voltage, $P_n = 10KW$ - rated active power, $V_{DC} = 800V$ - DC bus voltage, $f_g = 50Hz$ -grid frequency, $f_{sw} = 10KHz$ - switching frequency, $K_a = 20\%$ - attenuation factor is done.

Therefore, the base impedance and the base capacitance are:

$$Z_b = \frac{380^2}{10000} = 14.44\Omega$$

$$C_b = \frac{1}{2\pi * 50 * 14.44} = 220\mu F$$

The filter capacitance can be calculated by:

$$C_f = 0.05 * 22 * 10^{-6} = 11\mu F$$

To calculate the inverter-side inductor:

$$I_{\max} = \frac{10000\sqrt{2}}{3 * 220} = 21.4A$$

$$\Delta I_{Lmax} = 0.1 * 21.4 = 2.14A$$

$$L_i = \frac{800}{6 * 10000 * 2.14} = 6.23mH$$

For the grid-side inductor:

$$L_g = \frac{\sqrt{\frac{1}{0.2^2} + 1}}{11 * 10^{-6}(2\pi * 10000)^2} = 0.138mH$$

Now, we shall check if the system is within the stable region to avoid resonance:

$$\omega_{res} = \sqrt{\frac{0.138 * 10^{-3} + 6.23 * 10^{-3}}{0.138 * 10^{-3} * 6.23 * 10^{-3} * 11 * 10^{-6}}} = 25949rad$$

$$f_{res} = \frac{25949}{2\pi} = 4129.92Hz$$

$$10 * 50 < f_{res} < 0.5 * 10000$$

Therefore, the resonant frequency satisfies the equation, and the damping resistance can be calculated as follows:

$$R_f = \frac{1}{3 * 2\pi * 4129.92 * 11 * 10^{-6}} = 1.168\Omega$$

4.5 DC-Link Capacitor Selection

The DC link capacitor in a three-phase grid-connected inverter is a crucial component that serves multiple purposes, including:

- *Smoothing pulsating DC voltage:* The DC voltage often exhibits pulsations due to the inherent characteristics of these sources. The DC link capacitor acts as a reservoir, smoothing out these pulsations and providing a stable DC voltage to the inverter.
- *Energy storage:* During transient conditions, such as sudden changes in load, the DC link capacitor can provide or absorb energy to maintain the desired DC voltage level.
- *Filtering harmonics:* The switching operation of the inverter generates harmonic currents that can pollute the DC bus. The DC link capacitor helps to filter these harmonics, ensuring a cleaner DC supply for the inverter.
- *Limiting fault currents:* In the event of a fault, the DC link capacitor can limit the surge of fault current, protecting both the inverter and the connected equipment.

The selection of the appropriate DC link capacitor size is critical for the proper operation of the inverter. Several factors influence the capacitor selection, including:

1. Power rating of the inverter: The capacitor should be able to manage the maximum power output of the inverter.
2. DC voltage level: The capacitor must be rated for the DC voltage level of the system.
3. Permissible ripple current: The capacitor should be able to withstand the ripple current generated by the inverter's switching operation.
4. Desired ripple voltage: The capacitor selection determines the ripple voltage, which influences the inverter's efficiency and performance.
5. Transient response requirements: The capacitor should be able to support the transient energy demands of the system.
6. Environmental factors: The capacitor must be selected to withstand environmental conditions, such as temperature, humidity, and vibration.

There are two methods for calculating the DC-link capacitor value which we will discuss.

4.5.1 Method I

To calculate the DC link capacitor size, consider the following steps:

1. Determine the maximum DC power (P_{dc})
2. Calculate the RMS ripple current (I_{rms})

$$I_{rms} = m * \frac{P_{dc}}{2 * \sqrt{3} * V_{dc}} \quad (4.41)$$

3. Select an allowable ripple voltage (V_r): This is typically between 1% and 5% of the DC voltage.

4. Calculate the DC link capacitor capacitance (C_{dc}): Use the following formula:

$$C_{dc} = \frac{2 * P_{dc} * V_r}{I_{rms}^2 * \omega * V_{dc}} \quad (4.42)$$

where

- m is the modulation index
- V_{dc} is the DC voltage.
- ω is the angular frequency (2π *switching frequency)

4.5.2 Method II

Using capacitor's stored energy law:

$$C_{dc} = \frac{2 * P_{dc}}{V_{dc}^2 * f} \quad (4.43)$$

where

- f is the grid frequency
- V_{dc} is the DC voltage.
- P_{dc} is the maximum DC power.

4.5.3 Chosen Method

Two designs were done based on method II for both the low-rating system (1kW) and the high-rating system (10kW) to check its output.

Design Example - Low Power

A step-by-step procedure to obtain parameters of the filter with considering the following given data, needed for the filter design: $P_n = 1KW$ - rated active power, $V_{DC} = 200V$ - DC bus voltage, $f_g = 50Hz$ - grid frequency.

Therefore, the DC-link capacitance is equal to:

$$C_{dc} = \frac{2 * 1000}{200^2 * 50} = 1mF$$

Design Example - High Power

A step-by-step procedure to obtain parameters of the filter with considering the following given data, needed for the filter design: $P_n = 10KW$ - rated active power, $V_{DC} = 800V$ - DC bus voltage, $f_g = 50Hz$ -grid frequency.

Therefore, the DC-link capacitance is equal to:

$$C_{dc} = \frac{2 * 10000}{800^2 * 50} = 0.625mF$$

4.6 Component Selection

4.6.1 The Inverter Module

We have chosen an inverter module to begin with, to make the prototype of the main board of the AC/DC Rectification stage in our project.

We need to build a charger that can reach 7K watt to reach 22K watt by cascading, so we begin to build a prototype with lower rating to confirm that our topology is working well before evaluating it in high power rating.

Our prototype ratings are 1K watt with 200 V DC and 5 A at output, so we have chosen a 3-ph inverter ic_IKCM30F60GDXKMA1, its rating is 600V, 35A.

The Features

Fully isolated Dual In-Line molded module

- TRENCHSTOP™ IGBTs
- Rugged SOI gate driver technology with stability against transient and negative voltage
- Allowable negative VS potential up to -11V for signal transmission at VBS=15V
- Integrated bootstrap functionality
- Over current shutdown
- Temperature monitor
- Under-voltage lockout at all channels
- Low side emitter pins accessible for all phase current monitoring (open emitter)
- Cross-conduction prevention
- All six switches turn off during protection.
- Lead-free terminal plating; RoHS compliant
- Extremely low thermal resistance due to DCB

We bias the bootstrap with 15V using DC/DC transformer to make an isolation. Build the protection circuit from over-current and overheating. The Module can shutdown itself with the ITRIP pin that has a thermistor and send a signal (Volt Fault Out) to the micro-controller to alarm the fault.

4.6.2 The Current Sensor

The core of our topology is the closed loop feedback, so the measurement must be as accurate as we could be. We have chosen CAS transducer, the latest version of the LTS series. The nominal current is 25A to help us with future product.

The transducer has a multi-functional primary circuit that changes the nominal current lower to get more accuracy. In our Prototype we used the second technique that nominal current 12A. The

Number of primary turns	Primary nominal current rms I_{PN} [A]	Nominal* output voltage V_{out} [V]	Primary resistance R_p [mΩ] (typ.) at +25° C	Recommended connections
1	± 25	2.5 ± 0.625	0.24	
2	± 12	2.5 ± 0.600	1.08	
3	± 8	2.5 ± 0.600	2.16	

Table 4.2: Recommended connections for different sensitivities

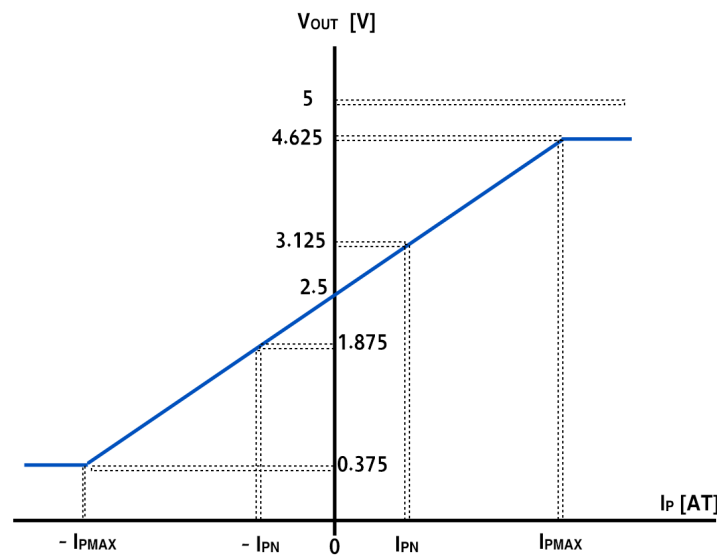


Figure 4.23: V_{out} versus I_p plot

most advantage is that the output signal does not need to re-scale or biasing and ready to send to the micro-controller.

4.6.3 The Voltage Sensor

We have chosen LV 25-P voltage transducer to get the voltage feedback

The Features

- Current equal to 10mA and Voltage ranging from 10V up to 500V

- Excellent accuracy
- Incredibly good linearity
- Low thermal drift
- Low response time
- High bandwidth
- High immunity to external interference
- Low disturbance in common mode.

This transducer needs an external circuit to re-scale and biasing the output signal before the controller, so we used an op-amp circuit after simulating it and get the desired output.

The transducer and the op-amp needed a positive and negative source power, so we used this topology to get the negative source.

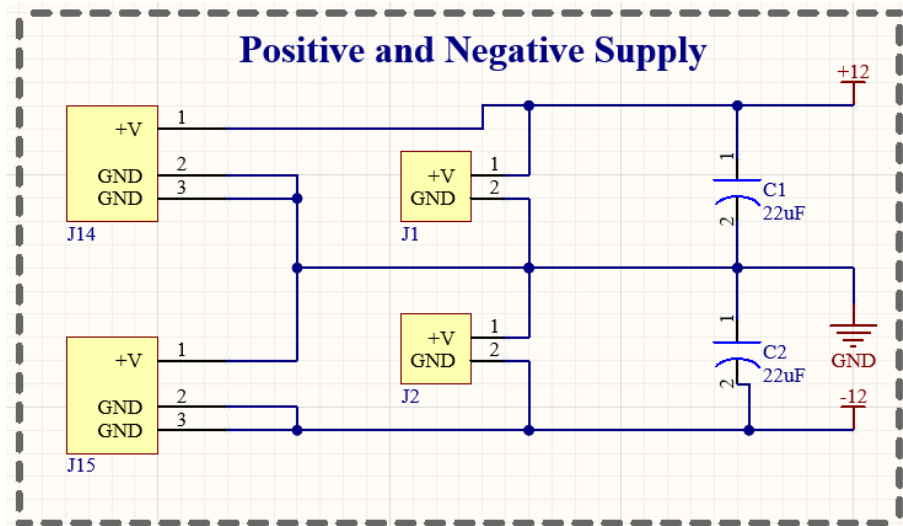


Figure 4.24: The schematic of the supply for the voltage sensor

The following figure shows the internal connection of the sensor:

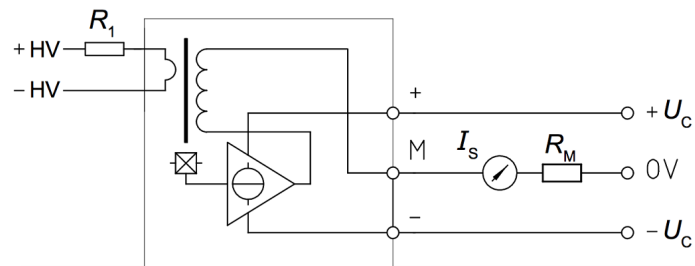


Figure 4.25: The internal connection of the voltage sensor

Primary Side (High Voltage):

- P1 and P2: terminals Connected to the voltage to be measured.
- R1 (External Resistor): Sets the primary voltage range corresponding to primary current of 10 mA.

Secondary Side (Low Voltage):

- +Vc: Connect this terminal to a positive power supply (5 to 15 V DC).
- -Vc: Connect this terminal to the negative power supply.
- OUT: signal to the micro-controller
- Rm (Scaling Resistor): Sets the output voltage range and sensitivity.

The resistors values can be calculated using the following equations:

$$R_m = \frac{V_{out}}{I_{out}} = 132\Omega \quad (4.44)$$

where

- V_{out} is the desired output voltage. (designed for 3.3V)
- I_{out} is the secondary circuit current.

$$R_1 = \frac{V_{in}}{I_p} = 50K\Omega \quad (4.45)$$

where V_{in} is equal to 500V and I_p is 10mA.

Interfacing with Micro-controller - Op-Amp Technique

In case of AC voltage measurements, DSP can not receive negative voltage So we need to shift the signal out of the transducer to the positive and re-scale it to get the desired output. Op-amp adder circuit will preform this operation to convert $(-3.3V, 3.3V)$ to $(0V, 3.3V)$.

Procedures to Design the Op-Amp circuit

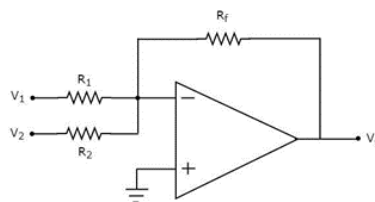


Figure 4.26: Op-amp circuit

where the first terminal represents the scale of input signal and the second terminal is the shift for scaled signal.

For input signal from sensor ,the AC voltage is first scaled to half, then shifted above x axis by this scaled value to obtain its peak positive value (V_{in}) and 0V.

$$-V_{out} = \left(\frac{R_f}{R_1} * V_{in} \right) + \left(\frac{R_f}{R_2} * V_2 \right) \quad (4.46)$$

for AC $V_{in} = 3.3V$

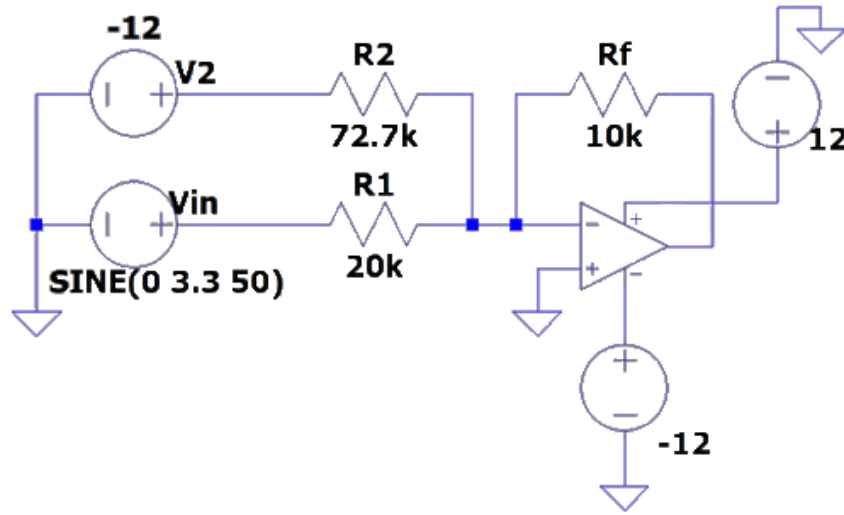


Figure 4.27: The circuit diagram of the op-amp

1. Scale the input signal to $\frac{1}{2}V_{in}$
 $\frac{R_f}{R_1} * V_{in} = 3.3/2$, assume $R_f = 10k\Omega$, so $R_1 = 20k\Omega$
2. Shift by $\frac{1}{2}V_{in}$
 $\frac{R_f}{R_2} * (V_2) = 3.3/2$, assume $V_2 = -12v$, so $R_2 = 72.7k\Omega$

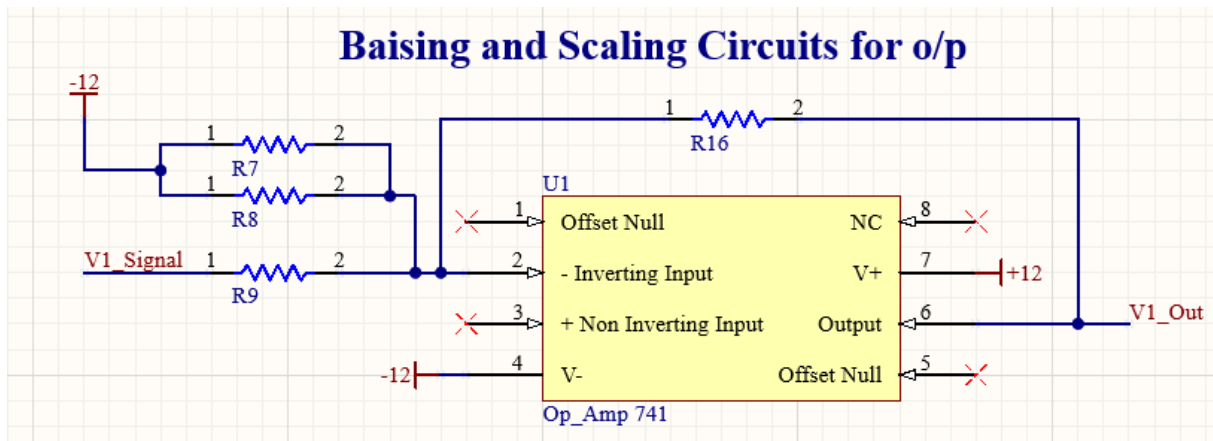


Figure 4.28: The schematic of the op-amp circuit

4.6.4 The Micro-controller

We have chosen to use DSP LaunchpadF28069M, because it is the easier controller to generate our model on it. We built a DSP interfacing with the inverter using optocoupler circuit to make the suitable isolation. For further references click here: [datasheet](#).

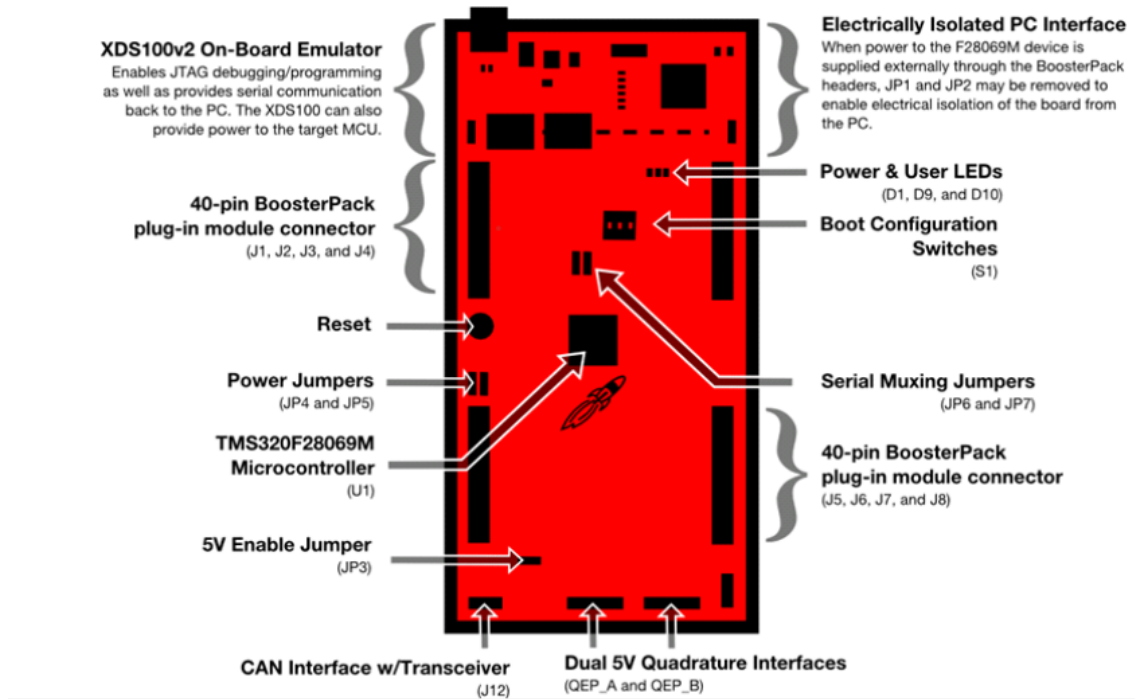


Figure 4.29: DSP LaunchpadF28069M

4.7 Hardware Design

Our hardware design process involved developing five specialized PCBs—Inverter module, DC-link board, current sensors board, voltage sensors board for feedback, and a micro-controller interfacing board. Altium Designer, version 2024, played a pivotal role in this endeavor, chosen over alternatives like Eagle for specific reasons.

Altium Designer’s selection hinged on its robust feature set. Its advanced tools facilitated precise design implementation, crucial for our intricate requirements.

Choosing Altium Designer over Eagle was a strategic decision based on its advanced features, multi-board design capabilities, documentation quality, community support, and scalability. This choice streamlined our PCB design for the inverter system efficiently.

4.7.1 The Inverter Module

This board is considered the main board as it interfaces with the micro-controller and the DC-link board, also it interfaces to collect the feedback from the current and the voltage sensors boards. This

board has indicating green LED to indicate the power connection, a red LED to indicate faults, several test points, IDC connecting cable to interface with the micro-controller and bootstrap circuits.

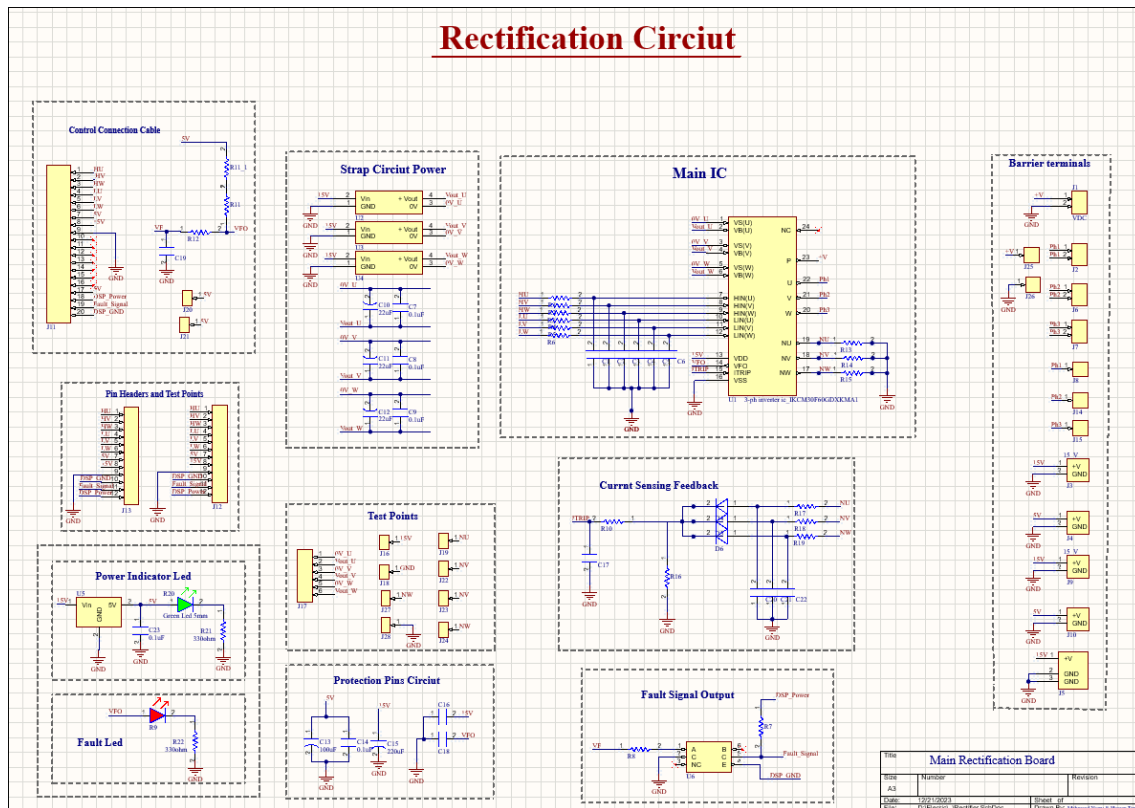
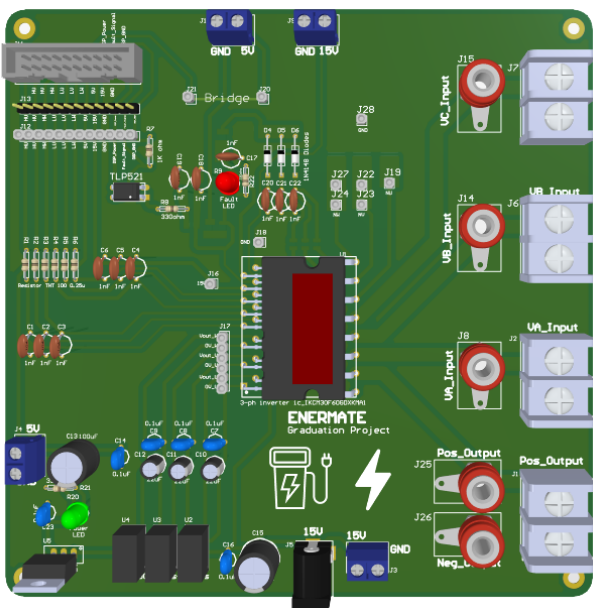
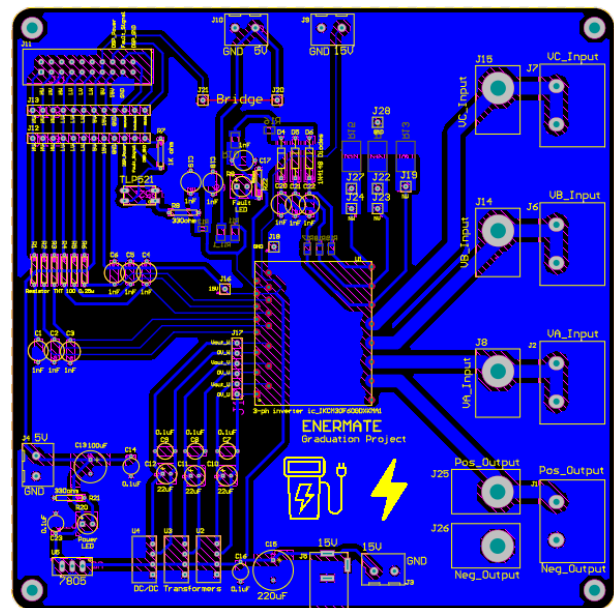


Figure 4.30: The schematic of the inverter module board



(a) Inverter module PCB 3D design



(b) Inverter module board - bottom layer

Figure 4.31: Inverter module hardware board design

4.7.2 DC-Link

According to our calculations that we have done in previous sections, we have designed a DC-Link to suit our project to literally link between the AC/DC Conversion and the DC/DC Conversion boards.

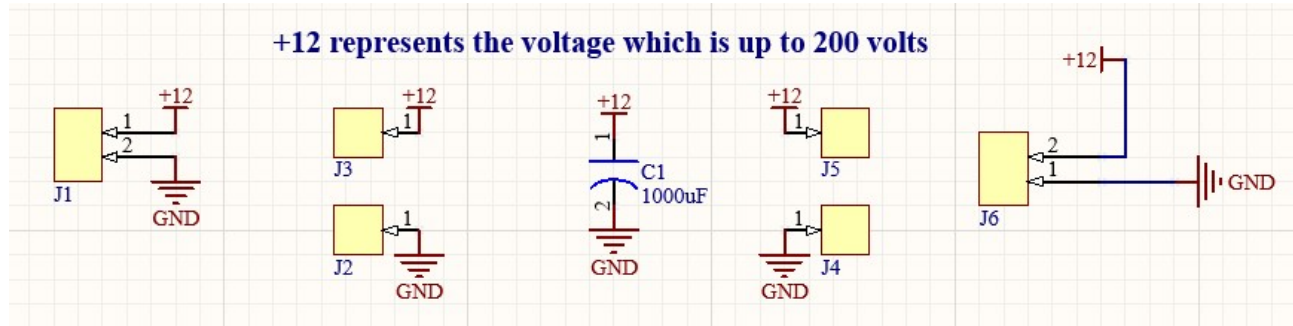
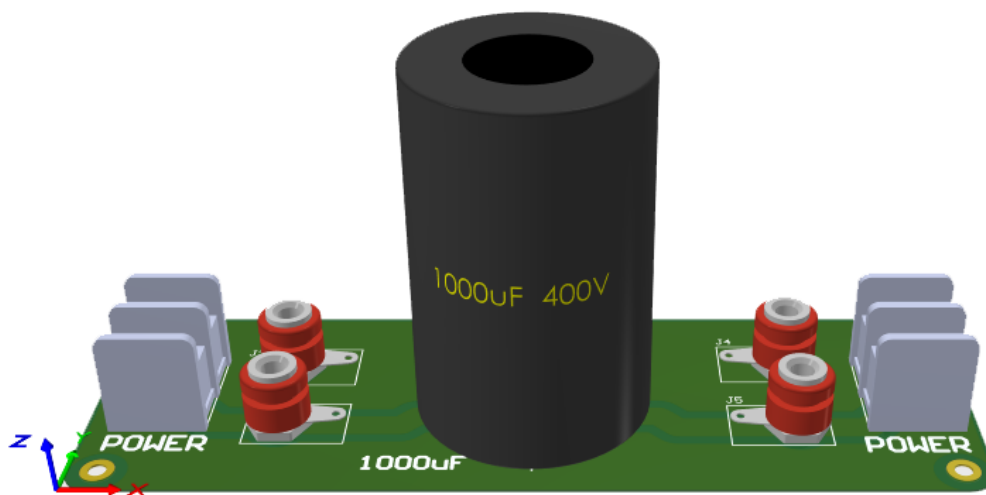
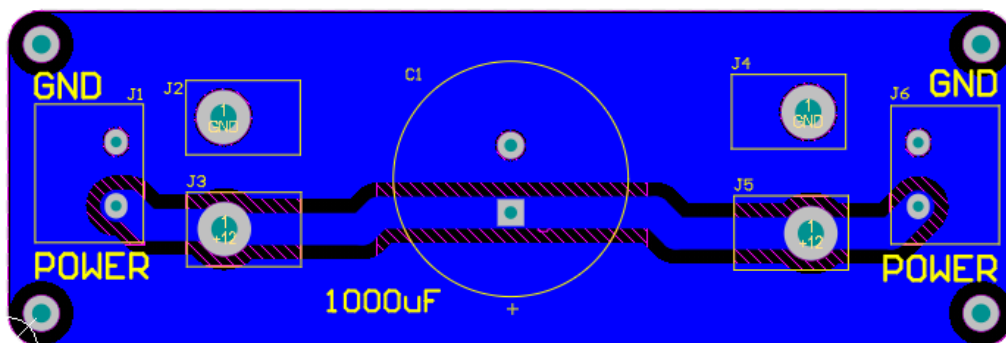


Figure 4.32: The schematic of the DC-link board



(a) DC-link PCB 3D design



(b) DC-link board - bottom layer

Figure 4.33: DC-link hardware board design

4.7.3 Current Sensors

This board is designed for three current sensors. It also has LED indicator to indicate the power connection. It interfaces with the main board to provide current feedback.

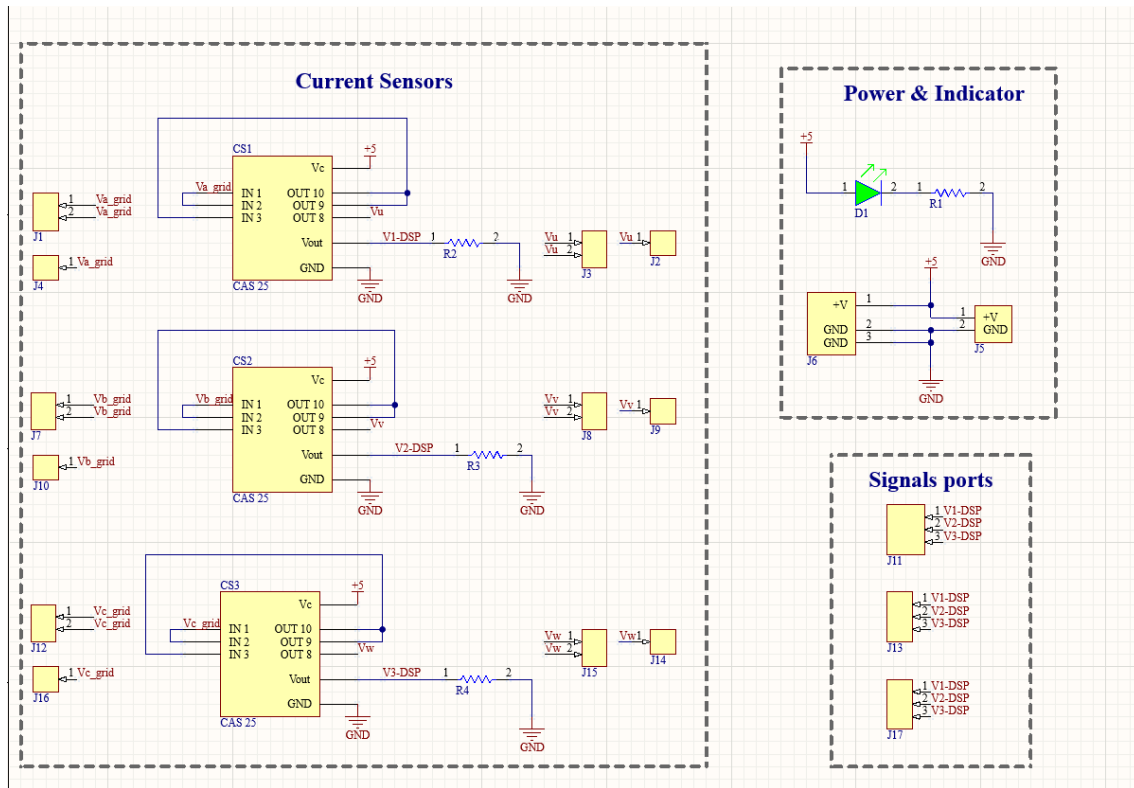
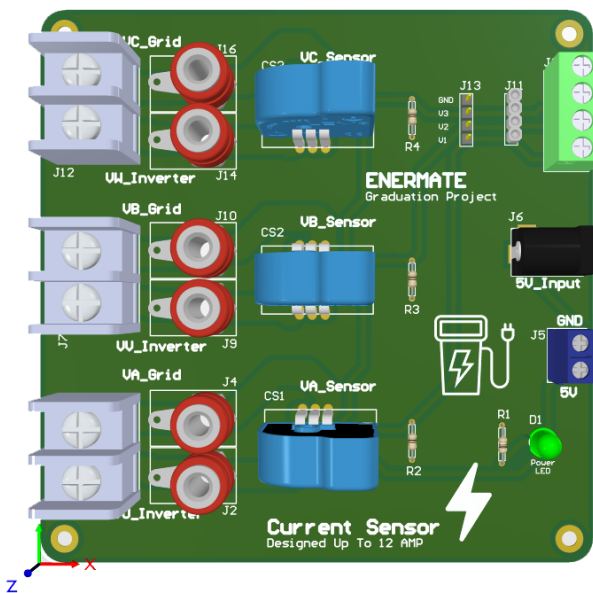
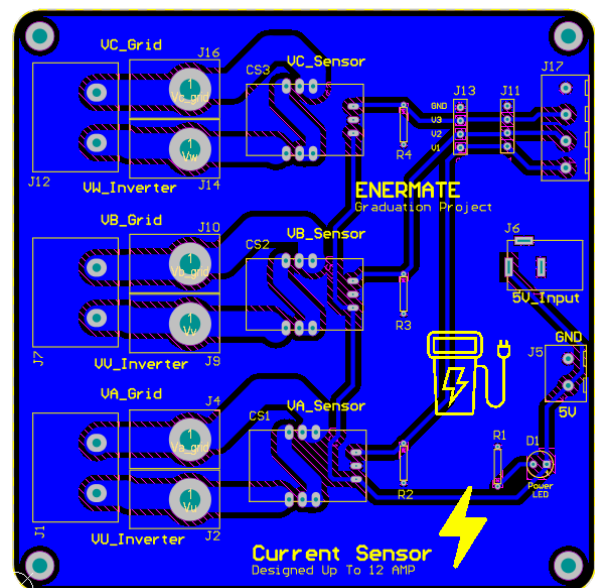


Figure 4.34: The schematic of the current sensors board



(a) Current sensors PCB 3D design



(b) Current sensors board - bottom layer

Figure 4.35: Current sensors hardware board design

4.7.4 Voltage Sensors

This board is designed for three voltage sensors, two of them will be used as a feedback of the input line voltage and the last one will be used as a feedback for the output DC voltage. It also has LED indicator to indicate the power connection.

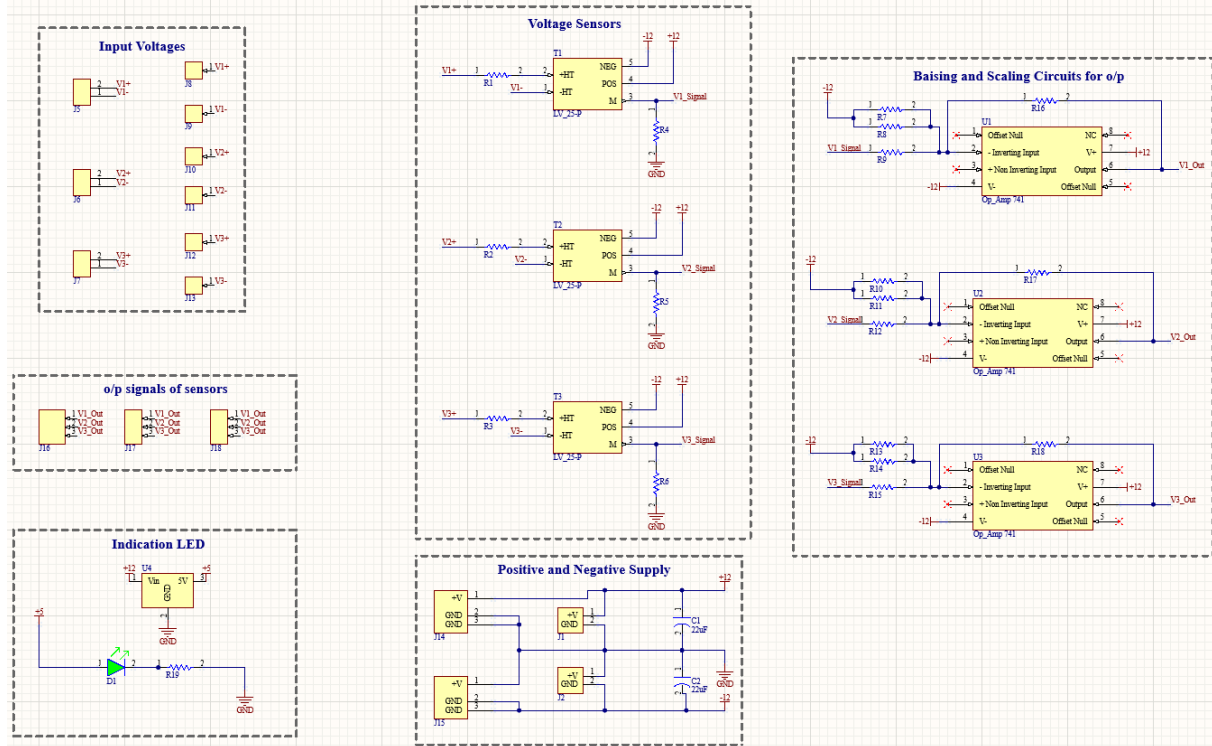
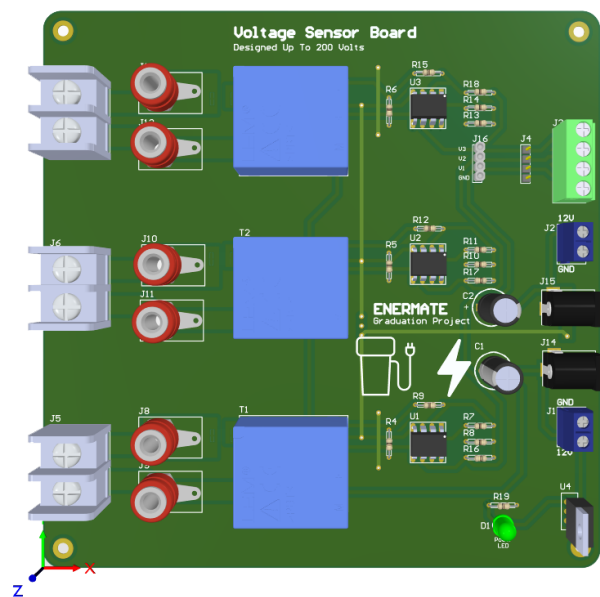
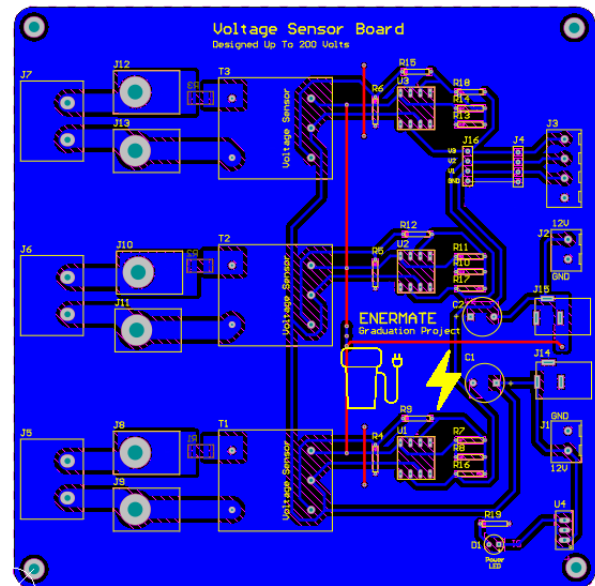


Figure 4.36: The schematic of the voltage sensors board



(a) Voltage sensors PCB 3D design



(b) Voltage sensors board - bottom layer

Figure 4.37: Voltage sensors hardware board design

4.7.5 Micro-controller Interfacing

This board acts as a shield for the DSP. It has several isolation optocouplers to protect the micro-controller from any fault.

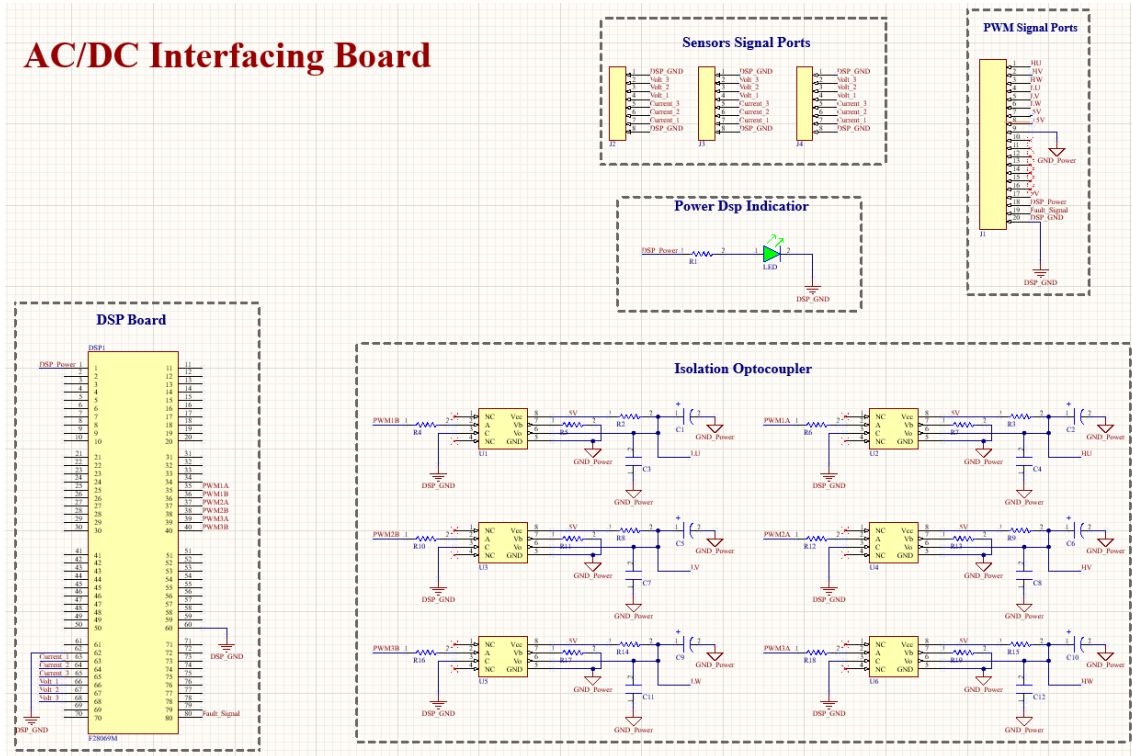
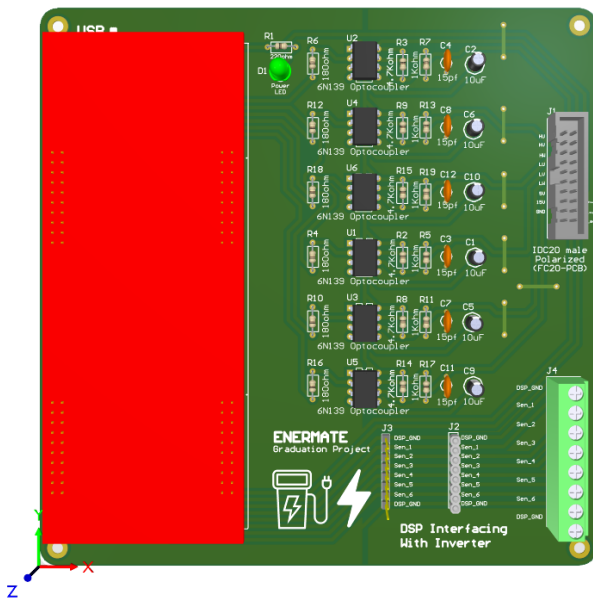
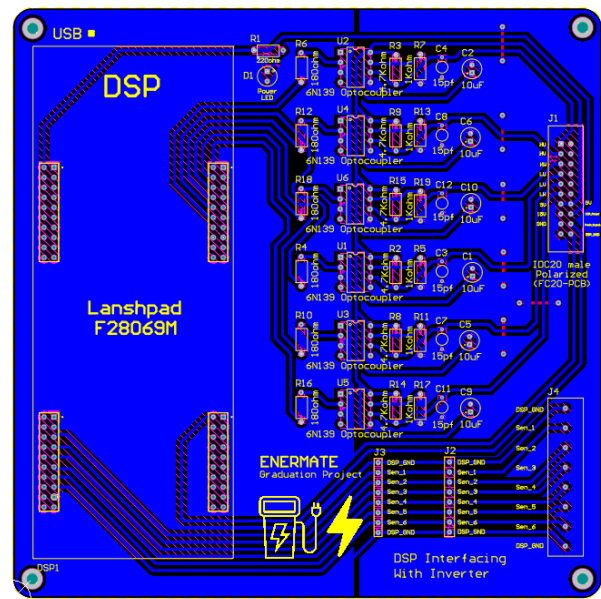


Figure 4.38: The schematic of the DSP interfacing board



(a) DSP interfacing PCB 3D design



(b) DSP interfacing board - bottom layer

Figure 4.39: DSP interfacing hardware board design

Bibliography

- [1] Steve Roberts. *AC/DC BOOK OF KNOWLEDGE*. RECOM Enginnering GmbH and Co.KG, 2018.
- [2] Saumitra Jagdale. Overview of ac/dc converters for fast-charging stations, 2023. [Online; posted 09-March-2023].
- [3] Manish Kumar Saini. Difference between half wave and full wave rectifier, 2023. [Online; posted 31-October-2023].
- [4] Harshada. Review of control techniques of three phase boost type pwm rectifiers. 2016.
- [5] Evren Isen and Ahmet Faruk Bakan. Development of 10 kw three-phase grid connected inverter. *Automatika*, 57(2):319–328, 2016.
- [6] A. Reznik, M. Godoy Simões, Ahmed Al-Durra, and S. M. Muyeen. Lcl filter design and performance analysis for small wind turbine systems. In *2012 IEEE Power Electronics and Machines in Wind Applications*, pages 1–7, 2012.
- [7] T. Simulator. Design of lcl filter for 3 phase grid connected inverter, 2020.
- [8] Min-Young Park, Min-Hun Chi, Jong-Hyoung Park, Heung-Geun Kim, Tae-Won Chun, and Em-Cheol Nho. Lcl-filter design for grid-connected pcs using total harmonic distortion and ripple attenuation factor. In *The 2010 International Power Electronics Conference - ECCE ASIA -*, pages 1688–1694, 2010.
- [9] A. E. W. H. Kahlane, Linda Hassaine, and M. Kherchi. Lcl filter design for photovoltaic grid connected systems. 2015.